University of Stavanger

Faculty of Science and Technology

MASTER'S THESIS

Study program/ Specialization: Petroleum Engineering/ Reservoir Engineering	Spring Semester 2018 Open
Author: Anna Bogunović Jakobsen	..... Writer's Signature

Faculty Supervisors:

Skule Strand
Tina Puntervold

Title of Thesis:

Adsorption of basic crude oil components onto carbonate chalk surfaces – effect on initial wettability.

Credits (ECTS):
30

Key Words: Smart Water Wettability Base number Acid number Adsorption Spontaneous imbibition Carbonates Chalk	Number of pages: 56 + Enclosure: 9 Stavanger June 14, 2018

Acknowledgements

I would like to express my gratitude to my supervisors Associate Professors Skule Strand and Tina Puntervold. They have both given me great advices and guidance throughout this thesis. I appreciate them for always keeping their doors open, ready to help and discuss my results. I am thankful for the opportunity to be a part of their smart water group at the University of Stavanger. It has been a very exciting journey.

I would also like to thank post doctoral fellow Iván Darío Piñerez Torrijos, for all the time he spent helping me with laboratory work, and his many advices regarding my thesis. Without his support – often outside his regular work hours – I could never have completed the labwork in time.

The work would not have been the same without my fellow laboratory companions; Kris, Miltos, Simen and Isaac. Thank you for providing a good work environment.

I also acknowledge the national IOR centre for my collaboration.

Finally, I would like to thank my family and boyfriend for all their support and encouragement.

Anna Bogunović Jakobsen

Abstract

The initial wetting of carbonate reservoirs is of great importance to the overall oil recovery and smart water processes. Crude oil is a complex mixture of organic components, and the polar components present in it can have a large impact on wettability. This study aims to improve the understanding of the initial wetting in chalk, caused by adsorption of polar organic oil components. The main objective is to obtain a better understanding of the adsorption of basic crude oil components onto carbonate chalk surfaces.

In this study two chalk cores were cleaned and flooded at 50 °C with a synthetic crude oil, containing a higher amount of bases compared to acids. The acid number (AN) and base number (BN) of the injected oil was known (AN=0.07 and BN=0.32), and effluent samples were collected and analyzed. Furthermore, the wettability of the cores after oil flooding was assessed. In order to see how the adsorption affected the initial wettability of the chalk cores, spontaneous and forced imbibition experiments were performed with formation water. This was followed by chromatographic wettability tests in order to confirm the wetting state. A 100% water-wet reference core was prepared for comparison purposes, and spontaneous imbibition by formation water and chromatographic wettability test was performed on the reference core.

The results showed that initially there was instantaneous adsorption of bases. The BN values reached equilibrium quite rapidly, before 2 PVs injected. The AN values obtained are within the area of uncertainty, possibly due to their relatively low concentration. Most likely the basic material is being complexated to the acidic components. Comparing the results to those of an oil with the same BN, but a higher AN, showed a large difference in adsorption. The adsorption of basic components, BN_{ads}, was quantified to 0.26 and 0.36, which are low values compared to those of AN_{ads} presented in previous studies. This strengthens the belief that the bases follow the acids. Spontaneous imbibition and chromatographic wettability tests compared to a 100% water-wet reference core, showed that the wettability was altered from very water-wet to quite water-wet.

Table of contents

List of Figures

List of Tables

Abbreviations and symbols

AN	Acid number
BN	Base number
CBR	Crude oil, brine and rock
EOR	Enhanced oil recovery
E	Overall displacement efficiency
E_D	Microscopic displacement efficiency
E_V	Macroscopic displacement efficiency
FI	Forced imbibition
IFT	Interfacial tension
I_{AH}	Amott Harvey index
IC	Ion chromatography
I_O	Displacement-by-oil-ratio
IOR	Improved oil recovery
I_W	Displacement-by-water-ratio
KOH	Potassium hydroxide
N_{ca}	Capillary number
NSO	Nitrogen, sulfur and oxygen
OOIP	Original oil in place
S_{or}	Residual oil saturation
S_{wi}	Irreducible water saturation
SK	Stevns Klint
SI	Spontaneous imbibition
μ	Viscosity
ρ	Density

1 Introduction

Since the start of Norwegian oil era in the mid 1960's, the petroleum industry has grown to become one of Norway's largest industries that now (2018) contribute to 14% of the Gross domestic product (GDP) and 40% of the export (Norwegian Petroleum, 2018). Much has changed since the start, both in terms of how exploration and production of oil and gas fields is planned, how the development work is done, and in terms of technology improvements that are used in the work. The low oil prices that emerged in 2014/2015[1] have also led to an increased focus on cost efficiency, and as a consequence, improved oil recovery from the reservoirs became even more important to make many of the planned projects sustainable. This has triggered increasing investment in finding new efficient and environmentally friendly methods for increasing oil recovery.

Carbonate rocks account for approximately 50% of the worlds proven oil reserves (Treiber et al., 1972), but the oil recovery in these reservoirs is relatively low, usually less than 30%. The fractured nature of these reservoirs is the main reason why the recovery is so low (Hognesen et al., 2005; Manrique et al., 2007). Studies evaluating the wetting state for different reservoirs from all over the world have also shown that most carbonate reservoirs seem to be neutral to oil-wet (Chilingar & Yen, 1983; Treiber et al., 1972). By altering the wettability towards a more water-wet system, capillary forces will increase and oil can more easily be produced by spontaneous imbibition. Hence, the enhanced oil recovery (EOR) potential in carbonate reservoirs is high.

Seawater is a smart water for carbonates, and has been injected with great success into the fractured chalk reservoir Ekofisk, situated in the Norwegians sector of the North Sea since the 1980´s. A prerequisite for a smart water process is that the system is initially mixed-wet, and therefore understanding the initial wetting is of high importance. Crude oil is the most important wetting parameter for carbonates (Austad, 2013). Several studies have been performed with the focus on the acid number (AN) of the crude oil, as the AN is found to have the largest impact on the initial wetting in carbonate. A higher AN was found to give a lower oil recovery (Standnes & Austad, 2000; Zhang & Austad, 2005). Hopkins et al. (2016) studied the adsorption of polar components onto carbonate surfaces, mainly with focus on the acidic material. The adsorbed acidic material was quantified as AN_{ads}.

Regarding the basic material in the crude oil however, much fewer studies have been performed so the knowledge is more limited. Experiments performed by Puntervold et al. (2007b) investigated the impact of basic components on the wetting properties of chalk by using an oil with a constant AN, and varying the AN/BN ratio. The wettability was found to increase as the amount of bases increased, what was explained by formation of acid-base complexes that prevent some of the carboxylic material to adsorb onto the surface. The present work is also devoted to the investigation of this topic.

[1] Historical inflation adjusted oil prces can be found at:
https://inflationdata.com/Inflation/Inflation_Rate/Historical_Oil_Prices_Table.asp

1.1 Objectives

This study focuses on optimized oil recovery in carbonate reservoirs by studying adsorption of polar organic components onto chalk surfaces and wettability alteration. The initial wetting of carbonate reservoirs is of high importance to the overall oil recovery. The main objective of this study is to understand the effect of how the basic components in the crude oil adsorb onto the rock surface. The chalk cores used in the study were cleaned and flooded at 50 °C with a synthetic crude oil, containing a much larger amount of bases compared to acids. The AN and BN of the oil entering the core was known (AN=0.07 and BN=0.32), and then after flooding the AN and BN values of the collected effluent are analyzed. The difference between these values represents the amount adsorbed by the core surface. Furthermore, the wettability of the cores after oil flooding was investigated. Spontaneous and forced imbibition was performed with formation water, to see how the adsorption affected the wettability. Chromatographic wettability test was also done to confirm the wetting state. Spontaneous imbibition and chromatographic wettability test was performed on a 100% water-wet reference core for comparison. The topic of this thesis supports study for smart water projects, where the goal is to manipulate the wettability. This study aims to improve the understanding of the initial wetting in chalk, caused by adsorption of polar organic oil components.

2 Fundamentals of oil recovery

2.1 Displacement forces

Several forces act on the fluid flow within a reservoir. The most important displacement forces within oil production are gravity forces, viscous forces and capillary forces (Morrow, 1979). The overall displacement during an EOR process can be looked at from different scales. The overall displacement efficiency *(E)* is defined as the product of macroscopic (volumetric) and microscopic displacement efficiencies, as shown by the following equation:

$$E = E_D E_V \tag{2.1}$$

where E_D is the microscopic displacement efficiency expressed as a fraction, and E_V is the macroscopic (volumetric) displacement efficiency also expressed as a fraction. The microscopic displacement expresses how the displaced fluid is mobilizing or displacing oil at pore scale. The magnitude of E_D reflects the magnitude of the residual oil saturation, S_{or}, in the regions that are in contact with the displacing fluid. The macroscopic displacement efficiency E_V is a volumetric interpretation of reservoir displacement and sweep efficiency. E_v measures how effectively the displacing fluids sweep out the volume of a reservoir. E_D is closely related to the wetting state of the rock, while E_V is mostly related to the mobility of displacing fluid. It is convenient that both E_D and E_V approach 1 to obtain a high displacement efficiency (Green & Willhite, 1998).

A spontaneous imbibition process is governed by gravity- and capillary forces. The interaction between these two forces is important, especially when the wettability approaches neutral wetting state, or when the interfacial tension (IFT) decreases. In case of a IFT reduction by several magnitudes, the gravity forces may dominate the flow pattern in the porous media.

2.1.1 Gravity forces

Gravity forces influence droplets of oil within a pore space. The main driving force is determined by the density of the fluids (Lake, 2010). The gravity forces play a significant role in multiphase systems where there may be large differences in densities of the fluids. The pressure difference between oil and water due to gravity is:

$$\Delta P_g = \Delta \rho g H \tag{2.2}$$

where

- ΔP_g pressure difference between oil and water due to gravity [Pa]
- $\Delta \rho$ density difference between oil and water [kg/m^3]
- g gravity acceleration, 9,81 [m^2/s]
- H height of the liquid column [m]

2.1.2 Viscous forces

During fluid flow through a porous media, viscous forces are reflected as the pressure drop occurring as a result of the flow through the medium. Viscous forces can be estimated by assuming laminar flow through the system and considering the porous media as a bundle of parallel capillary tubes. The pressure drop for a laminar flow through a single tube is then given by Poiseuille´s law, shown in equation 2.3 (Green & Willhite, 1998).

$$\Delta P = -\frac{8\mu L v_{avg}}{r^2 g_c} \tag{2.3}$$

where

ΔP	pressure drop across the capillary tube [Pa]
μ	viscosity [Pa·s]
L	length of the capillary tube [m]
v_{avg}	average flow velocity in the capillary tube [m/s]
r	radius of the capillary tube [m]
g_c	conversion factor

2.1.3 Capillary forces

Capillary forces are the main driving forces in fluid flow in porous media and govern the distribution of fluids within an oil reservoir. The forces depend on the dimensions and geometry of pore throats, wettability and the surface/interfacial tension generated by the fluids and rock of a given system. Capillary forces can act both in favor and disfavor of oil recovery efficiency. In fractured reservoirs, spontaneous imbibition of water due to strong capillary forces is considered as an important and necessary mechanism to attain high displacement efficiency (Lee, 2010). In a non-fractured reservoir on the other hand, strong capillary forces during waterflooding will trap oil and hence cause a high residual oil saturation (Anderson, 1987) .

Capillary pressure (P_c) can be described as the measurement of the force that draws fluid up in a tube or a capillary, as the pressure difference between two immiscible fluids (Zolotuchin & Ursin, 2000). The capillary pressure is found by the following equation:

$$P_c = P_{nw} - P_w \tag{2.4}$$

where P_{nw} is the pressure of the non-wetting phase at interface and P_w is the pressure of the wetting phase at interface.

The interface of two immiscible fluids in a capillary tube will usually be curved in the form of a meniscus, and the meniscal surface can be characterized by two radii as shown in Figure 1. The curvature is caused by the pressure difference between the two fluids, and the interface will always be convex towards the wetting fluid, which has the highest internal pressure. The Laplace equation (2.5) shows the relation between P_c and the different radii (Zolotuchin & Ursin, 2000):

$$P_c = \sigma(\frac{1}{R_1} + \frac{1}{R_2}) \tag{2.5}$$

where

σ interfacial tension between the non-wetting and wetting fluid [N/m]

R_1, R_2 principal radii of the interface curvature

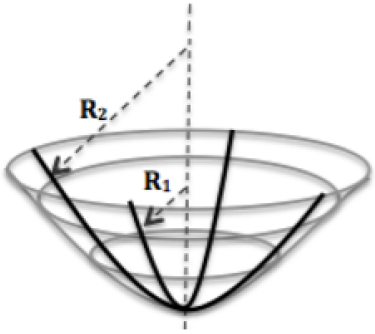

Figure 1: A meniscal surface and the main radii of its curvature, R_1 and R_2.

For a spherical oil droplet equal to pore size, or a hemispherical meniscus, one can say that $R_1=R_2$ and the pressure difference hence becomes $2\sigma/r$. The capillary pressure is given by equation 2.6 if we consider a cylindrical pore throat filled with oil and water, where water is the wetting fluid as illustrated in Figure 2.

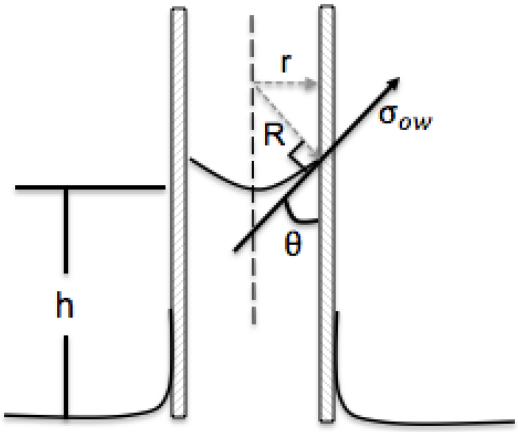

Figure 2: Idealized capillary pressure determination using cylindrical capillary tube model.

$$P_c = \frac{2\sigma_{ow}cos\theta}{r} \tag{2.6}$$

where

P_c capillary pressure

σ_{ow} the interfacial tension (IFT) between the non-wetting and wetting fluid [N/m]

r radius of the cylindrical pore channel

θ contact angle; defined as the angle between tangent to the oil-water surface in the triple-point solid-water-oil, measured through the water phase and the cylindrical wall

The capillary pressure is related to the relative wettability of the fluids (through θ), fluid/fluid IFT and the size of the capillary, r. The capillary pressure can be positive or negative; the sign simply expresses which phase has the lowest pressure. The phase that preferentially wets the capillary tube will always be the phase with the lowest pressure (Green & Willhite, 1998).

2.1.4 Fluid flow in porous media

Fluid flow through porous media is a substantial aspect to recover oil from reservoirs. Permeability is an important property that determines how the fluid flows through a porous medium. In an unfractured reservoir the fluid flow may be defined using Darcy´s law shown in equation 2.7 (Zolotuchin & Ursin, 2000):

$$q = \frac{kA}{\mu}\frac{dP}{dx} \tag{2.7}$$

where

q	fluid flow [m^3/s]
k	permeability [m^2]
A	cross-sectional area [m^2]
μ	viscosity [Pa·s]
$\frac{dP}{dx}$	pressure gradient [Pa/m]

2.2 Oil recovery

Oil production requires extensive planning both before and during the actual process of producing hydrocarbons. One important part of the planning process (prior to and during production) is to consider different recovery methods. Recovery methods are in general categorized into three stages; primary recovery, secondary recovery and tertiary recovery/enhanced oil recovery. Historically, these stages described the reservoir production chronologically. However, often we find that the recovery stages are not necessarily conducted in this order (Green & Willhite, 1998).

2.2.1 Primary recovery

The process in which one uses only naturally present energy in the production process is called primary recovery. This is usually the first production stage. In this stage, the natural energy of the reservoir is used to extract oil from the reservoir to production wells. Examples of natural energy sources are solution gas, water influx, gas cap drive or gravity drainage (Green & Willhite, 1998). An inevitable disadvantage of the primary recovery methods is gradual and rapid decrease in the reservoir pressure. This can lead to development of solution gas drive and to unacceptable low production rates (Zolotuchin & Ursin, 2000). When only primary oil recovery is used, the recovery is typically 10 to 30% of the original oil in place (OOIP) (Castor et al., 1981).

2.2.2 Secondary recovery

Secondary recovery is traditionally initiated when the primary recovery is declining. To produce more oil or to provide a more efficient displacement, the reservoir pressure must be maintained by injection of another fluid. The injected fluid is normally water or gas. Out of these, water flooding with seawater is the most common method, and the reason why water flooding previously was used as a synonym for secondary recovery. Gas injection during the secondary recovery would be either into a gas cap for pressure maintenance or gas-cap expansion, or into oil-column wells to displace oil immiscibly according to relative permeability and volumetric sweep considerations (Green & Willhite, 1998). Maximum recovery factor from the reservoir cannot be provided by secondary methods alone. The three main factors for this are reservoir heterogeneity, problems related to well siting and spacing and unfavorable mobility ratio between the displacing and displaced fluids. All of the three factors result in a low volumetric (macroscopic) sweep efficiency (Zolotuchin & Ursin, 2000). After secondary recovery, around 30 to 70% of OOIP is left unproduced (Bavière, 1991).

2.2.3 Tertiary recovery/Enhanced oil recovery

Traditionally tertiary oil recovery methods are initiated when secondary recovery becomes uneconomical. However, the reality is that the three oil recovery stages are not necessarily conducted in chronological order. For example for some heavy oils, a method considered tertiary might be the first and the only method used. In other cases, tertiary recovery methods are often applied right after primary recovery. Due to this, the term “tertiary oil recovery” is usually replaced by the term “Enhanced Oil Recovery”, abbreviated EOR. Another term used is “Improved Oil recovery” (IOR), which includes EOR but also includes a broader spectrum of activities such as reservoir characterization, reservoir management and infill drilling (Green & Willhite, 1998).

EOR combines methods used to increase ultimate oil recovery by injecting suitable fluids that are not normally present in the reservoir. Examples of such fluids are chemicals, solvents, oxidizers and heat carriers, which are injected in order to induce new mechanisms for producing the remaining oil (Abdelgawad & Mahmoud, 2014). EOR processes can be divided into five broad categories: thermal, miscible, chemical, immiscible gas drives and other processes. The methods are described in Table 1.

Table 1: Classification of EOR processes (Taber et al., 1997; Thomas, 2008).

Chemical	Surfactant Alakaline Polymer Micellar Emulsion
Miscible	Slug Process Enriched Gas Drive Vaporising Gas Drive CO_2 Miscible N_2 Miscible Alcohol
Immiscible gas drives	CO_2 Flue Gas Inert Gas
Thermal	Hot Water In-Situ Combustion Steam Electrical Heating
Other	Microbial Enhanced Oil Recovery Foam Water Alternating Gas Low Salinity Water Injection

Recently, wettability alteration has been suggested as a new EOR mechanism. Wettability alteration increases capillary forces and improves microscopic sweep efficiency, and methods are described in Table 2. In order to get a more economical and efficient EOR project, it is wise to include an EOR strategy already during the initial planning process of a well. The downside is that many of the processes are quite expensive. Water flooding used to be characterized as a secondary oil recovery process since no special EOR chemicals were injected. During the last 25 years several laboratory studies has been executed by numerous research groups on different crude oil, brine and rock (CBR) systems. It has been verified that injected water, which has a different composition than the initial formation water, can disturb the established chemical equilibrium of the CBR-system. Today one might say that water flooding is one of the most cost efficient and adaptable EOR methods (Austad, 2013).

Table 2: Suggested EOR process by water base wettability alteration.

Wettability Alteration	Smart Water Seawater/modified Seawater (in Carbonates) Low Salinity (in Sandstones)

2.2.4 Smart water

Several enhanced oil recovery processes have been developed during the recent years. One of them is called smart water. During million of years, a chemical equilibrium has been established between the crude oil, brine and rock (CBR) system. The distribution of formation water and oil in the pores of the rock is then fixed at given saturations of oil and water. The distribution of oil and water in the porous system is linked to the contact between the rock surface, and the oil and brine, i.e. the wetting properties. The idea of smart water is to modify wetting conditions by injecting a fluid with a modified composition. The target is to change the equilibrium of the initial CBR-system, and hence alter the wettability. This has a favorable effect on the capillary pressure and relative permeability of oil and water in regard to the oil recovery. Oil then becomes more mobile and can be removed more easily, as illustrated in Figure 3. The technique is environmentally friendly and has no expensive chemicals added so it is also economical. Studies so far have shown no injection problems. For economical reasons, it would be preferential to flood with a smart water from the beginning of the water flooding process (Austad, 2013). For the smart water process it is essential to understand the initial wetting of the system, and the factors influencing it.

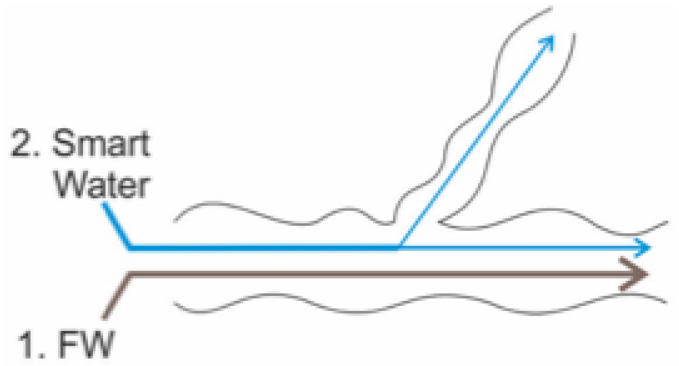

Figure 3: Illustration of wettability alteration by smart water (Smart water group, 2018)

2.3 Carbonate reservoirs

It is documented that carbonate rocks account for approximately 50% of the worlds proven oil reserves (Treiber et al., 1972). Generally carbonate reservoirs are naturally fractured and characterized by heterogeneous porosity and low permeability distributions. The overall permeability range is 1-10 mD. The oil recovery is predictably low compared to sandstones (less than 30%), mainly due to the fractured nature of these reservoirs (Hognesen et al., 2005; Manrique et al., 2007). Studies evaluating the wetting state for different reservoirs from all over the world indicate that most carbonate reservoirs seem to be neutral to oil-wet (Chilingar & Yen, 1983; Treiber et al., 1972).

2.3.1 Carbonate rocks

Carbonates are sedimentary rocks formed by the anionic complex CO_3^{2-}, together with divalent metal ions such as for example Ca^{2+}, Mg^{2+}, Fe^{2+}, Mn^{2+}, Zn^{2+}, Ba^{2+}, Sr^{2+} and Cu^{2+} (Ahr, 2008). The carbonate sediments are produced in shallow warm oceans where they are precipitated out of seawater, or by biological extraction of calcium carbonate from seawater to form skeletal material. The result is sediments composed of particles with various shapes, sizes and mineralogy mixed together to form a multitude of chemical compositions, textures

and pore-size distributions (Lucia, 1999). If the sediment material is fragmented, the rock is classified as a clastic rock, meanwhile a non-clastic rock will consist mainly of intact sediments. Limestone and dolomite, carbonate rocks in which hydrocarbons are often discovered, are hard to classify as they can be classified as either clastic or non-clastic (Skinner & Porter, 1992).

Geologists generally classify rocks consisting of more than 50% carbonate minerals as a carbonate rock. Typically carbonate rocks are composed of either calcite ($CaCO_3$), dolomite ($MgCa(CO_3)_2$) or a combination of these minerals. Limestones are best defined as sedimentary rocks containing more than 50% of the mineral calcite, and contrary dolomite (also called dolostone) is defined as a sedimentary rock containing more than 50% of the mineral dolomite (Mazzullo et al., 1992). The porosity of most carbonate reservoirs ranges from 5% to 15%, and it decreases with depth (Ahr, 2008). Carbonates differ from sandstones in several ways. An important difference is that sandstones are the result of transported detritus, whereas carbonates on the contrary are formed mainly from the remains of plants and animals, that lived near the place of deposition (Mousavi et al., 2013).

Chalk is classified as a special type of bioclastic limestone. It is composed of the tiny skeletal parts of pelagic coccolithophorid algea, called coccoliths (Zolotukhin and Ursin, 2000). These algae consist of ring structures, typically with dimensions 3-15μm in diameter (Puntervold, 2008). Figure 4 is a scanning electronic miscroscopy (SEM) photo clearly showing the ring structure and ring-fragments, both intact and non-intact. Chalk is characterized as highly porous, with several tens of porosity. This is much higher than the normal range for carbonate reservoirs. The Ekofisk and Valhall formation are examples of chalk reservoirs, with the porosity as high as 50% (Hardman, 1982). The matrix consists primarily of micro-interparticle pores (between whole and fragmented skeletons of coccolithophorids) and micro-intraparticle pores (in the centre of the coccolithic rings). Due to the microscopic size of the constituents, chalk has a low permeability (Milter, 1996).

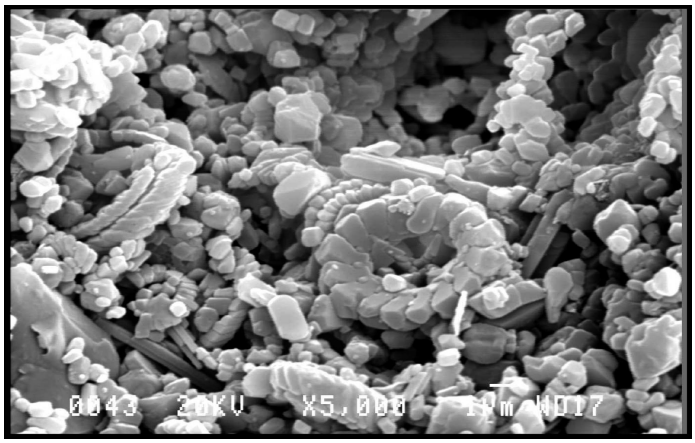

Figure 4: Scanning electronic microscopy (SEM) picture showing coccolithic ring structures in chalk (Puntervold, 2008).

3 Wettability

One can define wettability as ”the tendency of one fluid to spread or adhere to a solid surface in the presence of other immiscible fluids” (Anderson, 1986a). The limitation of this definition is that it does not take into account the interaction of the three phases in a CBR-system, as each phase has several components that can affect the wetting (Drummond & Israelachvili, 2002). Wettability is a major property that controls multiphase flow, location and fluid distribution in a reservoir. The initial wettability is of crucial importance, as it will affect properties such as capillary pressure, relative permeabilities, irreducible saturation and waterflood performance. It is difficult to give a general definition of wettability

3.1 Wettability classification

In a CBR-system, a reservoir rock can be characterized as water-wet, oil-wet, mixed-wet or fractional wettability (Donaldson & Alam, 2013). In a water-wet condition, at irreducible water saturation (S_{wi}) water will exist as a continuous phase throughout the whole matrix. Water will occupy the smaller pores, and the oil saturation will be high enough for also the non wetting phase (the oil) to exist as a continuous phase through the larger pores of the rock. As the water saturation increases, the non-wetting phase will quickly become discontinuous and oil will be presented in the center of larger pores as droplets. This is illustrated in Figure 5a.

In an oil-wet condition, the position of water and oil in the porous rock is reversed. Oil will occupy the smaller pores, and also the rock surfaces of the larger pores. Water will be present in the center of the larger pores. If the water saturation is high (near the S_{or}), water will exist as a continuous phase in the center of the larger pores. If the water saturation is decreased, water will be in the center of the larger pores isolated and resting on a film of oil (Figure 5b) (Donaldson & Alam, 2013).

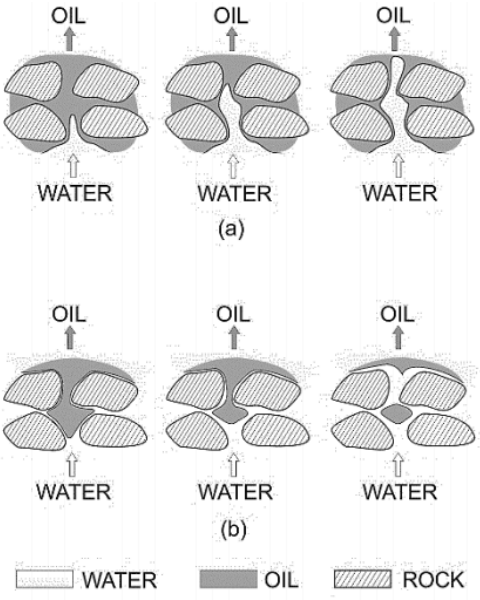

Figure 5: Displacement of oil by water (a) oil-wet sand, and (b) water-wet sand. Redrawn after Craig (1980).

When a system does not have a strong preference towards oil or water, it is characterized as an intermediate or neutrally wetted system. Another classification of wettability distinguishes between homogeneous (uniform) and heterogeneous wettability. Strongly water-wet, oil-wet and neutrally wet systems all belong to the category uniform wettability (Anderson, 1986a).

The term fractional wettability relates to a heterogeneous (non-uniform) system where the surfaces can be both water-wet and oil-wet. The preferential wetting is randomly distributed throughout the rock (Donaldson & Alam, 2013). This term must not be mistaken with another heterogeneous term introduced by Salathiel (1973); mixed wettability. In a mixed wet condition, the fine pores and grains are preferentially water-wet while the surfaces of the larger pores are strongly oil-wet. The larger oil-wet pores are filled with oil and form a continuous path throughout the whole length of the core. This way water can displace oil from the larger pores and capillary forces will hold little or no oil in the smaller pores. This explains why mixed wettability is characterized by such a low S_{or} (Salathiel, 1973).

3.2 Wettability measurements methods

Several methods can be used to evaluate the wetting of a fluid system, both qualitative and quantitative. Quantitative methods are contact angle measurements, Amott (imbibition and forced displacement), the USBM method and chromatographic wettability test. In addition, quantitative methods include: measurements of the imbibition rates, microscope examination, flotation, glass slide method, relative permeability curves, capillary pressure curves, capillarimetric methods, displacement capillary pressure, permeability/saturation relationships, reservoir logs, nuclear magnetic resonance and dye adsorption.

When characterizing wettability, one must ensure that the method used does not change the wetting condition of the surface during the measurement procedure. The minerals of the rock, and hence also the pores have various surface characteristics, including for example chemical properties that can influence the wettability. Also, the oil composition involving acidic and basic material can be of influence (Hopkins, 2016). No single accepted method exists, but the most general methods are the qualitative ones (Anderson, 1986b). The following section will describe the most classical methods.

3.2.1 Contact angle measurement

The surface energies in a rock/brine/oil system may be illustrated by Young´s equation (3.1) and is illustrated in Figure 6.

$$\sigma_{ow} cos\theta = \sigma_{os} - \sigma_{ws} \tag{3.1}$$

where

- θ contact angle, the angle of the water/oil/solid contact line (usually measured through the water phase)
- σ_{ow} interfacial tension between oil and water
- σ_{os} interfacial tension between oil and solid
- σ_{ws} interfacial tension between water and solid

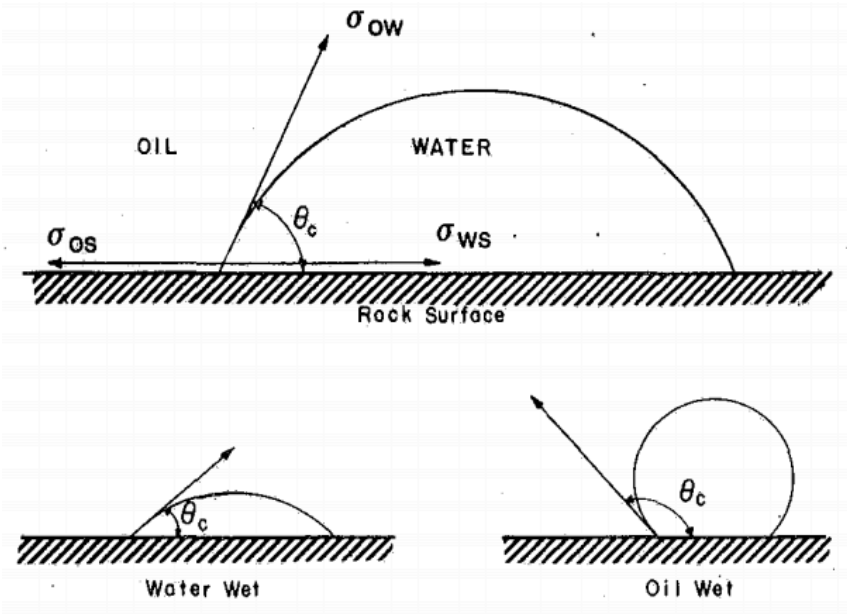

Figure 6: Wettability of an oil/water/rock system (Anderson 1986b).

When pure brines and artificial cores that have smooth surfaces are used, contact angle measurement is the best wettability measurement method. The method shows the equilibrium between the interfacial tension of the two liquids towards each other and toward the solid. Several methods of contact angle measurement exist, such as the tilting plate methods, sessile drops or bubbles, vertical rod methods, tensiometric methods, cylinder methods and capillary rise method. Among these, the method most generally utilized in the petroleum industry is the sessile drop method. This method makes contact angle measurement in a direct way. If the contact angle is less than 90° the surface is preferentially water-wet, and water occupies the smaller pores and is the spreading fluid. If the angle is greater than 90° the smaller pores are occupied by oil and the surface is preferentially oil-wet. When the rock has no strong preference for either fluid, the rock is intermediate or neutrally wet (θ=90°) (Anderson, 1986b)

3.2.2 Spontaneous imbibition

Spontaneous imbibition (SI) is particularly of importance to oil recovery from fractured reservoirs (Morrow & Mason, 2001). By definition, spontaneous imbibition is the process where a wetting fluid is drawn into a porous medium by capillary forces. SI measurements are therefore directly related to the capillary pressure. SI is an experimental procedure that measures both the rate and the total recovery of oil when water spontaneously imbibes into the pores and displaces oil. The procedure is efficient and provides relative wettability measurements for systems with various degrees of water wetness (Morrow, 1979). Also the form of the imbibition curve can be of importance. Characterization of wettability by imbibition is made by comparing to reference samples that have close to perfect wetting conditions (Morrow & Mason, 2001). Figure 7 shows an illustration of two cases of SI. The steeper (blue) curve represents a more piston-like displacement and a higher ultimate recovery than the slower rising (red) curve. The blue curve also indicates a more water-wet system.

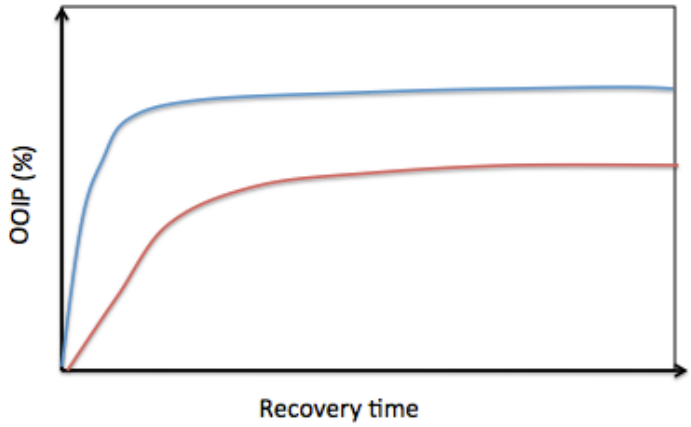

Figure 7: Principle sketch of results from a spontaneous imbibition, blue curve presenting a steep, rapidly recovery and red curve presents a slower and ultimate lower recovery.

3.2.3 Amott method

In the Amott method (Amott 1959) SI and forced displacement (by centrifuging) are combined to measure the average wettability. The method is based on the principle that the wetting fluid will imbibe spontaneously into the core and displace the non-wetting fluid (Anderson, 1986b). The ratio of SI to forced imbibition is used to reduce the influence of other factors, such as relative permeability, viscosity and S_{wi} of the rock (Anderson, 1986b).

The result of the Amott test is the "displacement-by-oil-ratio", I_O, and the "displacement-by-water-ratio", I_W. These two ratios are reported separately as shown by equation 3.2 and 3.3:

$$I_W = \frac{\Delta S_{WS}}{\Delta S_{WS} + \Delta S_{WF}} \tag{3.2}$$

$$I_O = \frac{\Delta S_{OS}}{\Delta S_{OS} + \Delta S_{OF}} \tag{3.3}$$

where

ΔS_{WS} saturation change during spontaneous imbibition of water
ΔS_{WF} saturation change during forced imbibition of water
ΔS_{OS} saturation change during spontaneous imbibition of oil
ΔS_{OF} saturation change during forced imbibition of oil

Cores that are strongly preferentially water-water will show I_W approaching 1.00 and I_O of zero. On the other hand, cores that are strongly preferentially oil-wet will give the opposite results. Both ratios are zero for neutral wettability (Amott, 1959).

The Amott-Harvey method is a modification of the Amott test method, and this method is more commonly used. The method results in the Amott-Harvey index, I_{AH}, which is the

difference between the two Amott displacement indexes, shown by equation 3.4 (Anderson, 1986b).

$$I_{AH} = I_O - I_W \tag{3.4}$$

The Amott-Harvey test-cycle is divided into five segments. These are illustrated in Figure 8, and the steps are:

1. Primary drainage of water by oil to establish initial water saturation, S_{wi}
2. Spontaneous imbibition of water
3. Forced imbibition of water
4. Spontaneous imbibition (drainage) of oil
5. Forced imbibition (drainage) of oil

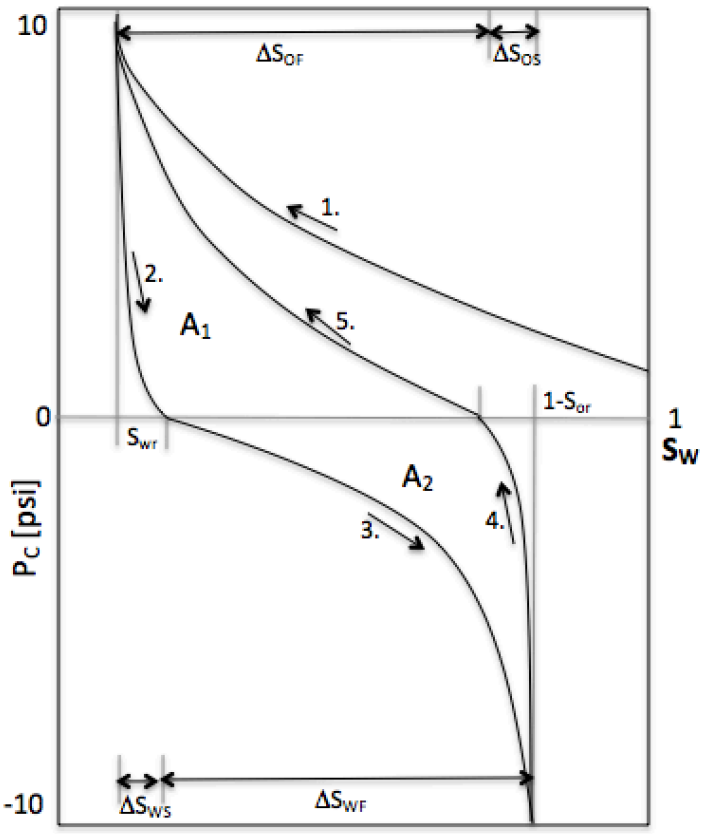

Figure 8: Capillary pressure curve for Amott and Amott-Harvey method.

The Amott-Harvey index ranges from -1 for a completely oil-wet system to +1 for a completely water-wet system. Cuiec (1984) extended the index range by characterizing $-1 < I_{AH} < -0.3$ as an oil-wet system, $-0.3 < I_{AH} < 0.3$ as an intermediate-wet system and $0.3 < I_{AH} < 1$ as a water-wet system. Disadvantages with the Amott methods are that they can be time-consuming. The methods are insensitive near neutral wettability (Anderson, 1986b), and it is reported that they do not distinguish well enough between different degrees of strong water wetness (Ma et al., 1999; Morrow, 1990)

3.2.4 United states bureau of mines (USBM) method

The USBM method also measures the average wettability of the core, and the measuring principle of the method is similar to the Amott method. The advantage with this test is that it is time efficient and sensitive close to neutral wetting. One disadvantage of the test is that it can measure only plug-size samples since the samples need to be spun in a centrifuge (Anderson, 1986b). USBM test (Donaldson et al., 1969) compares the work done by one fluid to displace the other by measuring the area in the two regions of capillary pressure curves produced during the forced drainage and imbibition processes, Figure 8. Due to favorable free-energy change, the work required for the wetting fluid to displace the non-wetting fluid from the core is less than the work required for the opposite displacement. The required work is found to be proportional to the area under the capillary pressure curve. Hence, if a core is water-wet, the area under the brine-drive capillary pressure curves (when water displaces the oil) is smaller compared to the area under the capillary pressure curve for the opposite displacement (Anderson, 1986b).

The USBM method uses the ratio of the areas under the two capillary curves (A_1 and A_2) to calculate the wettability index (I_{USBM}), as defined according to equation 3.5:

$$I_{USBM} = \log\left(\frac{A_1}{A_2}\right) \tag{3.5}$$

where A_1 is the area between the forced drainage curve and the saturation axis and A_2 is the area between the forced imbibition curve and the saturation axis, as shown in Figure 8. When I_{USBM} is greater than zero, the core is water-wet, and when I_{USBM} is negative, the core is oil-wet. When I_{USBM} has values close to zero it means the core is neutrally wet (Anderson, 1986b).

3.2.5 Chromatographic wettability test

Strand and colleagues at the University of Stavanger and Bergen developed the chromatographic wettability test in 2006 (Strand et al., 2006). The test analyzes surface reactivity by measuring the amount of water-wet carbonate surface. The experiment can be run at S_{or} and 25 °C, but can also be done on 100% saturated cores. The method is based on chromatographic separation between the two water-soluble ions; sulfate SO_4^{2-}, and thiocyanate SCN^-. As SO_4^{2-} has a higher affinity towards the water-wet areas of the carbonate surface, the ions will adsorb onto the water-wet surface. Thiocyanate is a tracer that has no affinity for the carbonate surface, and it is also not expected to engage in any chemical interactions within the core. It is therefore chosen to keep track of the fluid front. An illustration of the adsorption process to the surface for different wettabilities is illustrated in Figure 9.

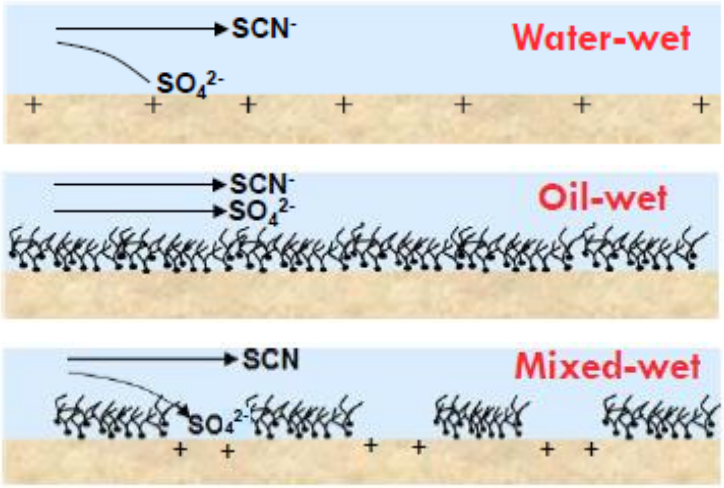

Figure 9: Adsorption of SO_4^{2-} onto a water-wet, oil-wet and mixed-wet surface (Shariatpanahi, 2012)**.**

The ion chromatography (IC) measures the concentrations of effluent samples. The chromatographic analysis of the anions of the effluent, will show that the sulfate concentration appears delayed compared to the thiocyanate concentration. The area between these two effluent concentration curves, is directly proportional to the water-wet surface as the separation only takes place at the water-wet areas of the surface. The area is illustrated in Figure 10. The wettability index (WI) is the defined as:

$$WI = \frac{A_{Wett}}{A_{Heptane}} \tag{3.6}$$

where

A_{Wett} the area ratio between the thiocyanate and sulfate curves

$A_{Heptane}$ the area of a reference sample containing 100% heptane, and is assumed to be a completely water-wet system.

The areas are calculated using the trapezoidal method of numerical integration. The scaling of the WI runs from 0 to 1, where 0 is completely oil-wet, 0.5 is neutral wettability and 1 is completely water-wet. The advantage of the chromatographic wettability test is that it is very useful close to neutral wetting conditions, which is usually the case for carbonates. The method is also time-efficient. A disadvantage of the test is that is can only be used on carbonates (Strand et al., 2006).

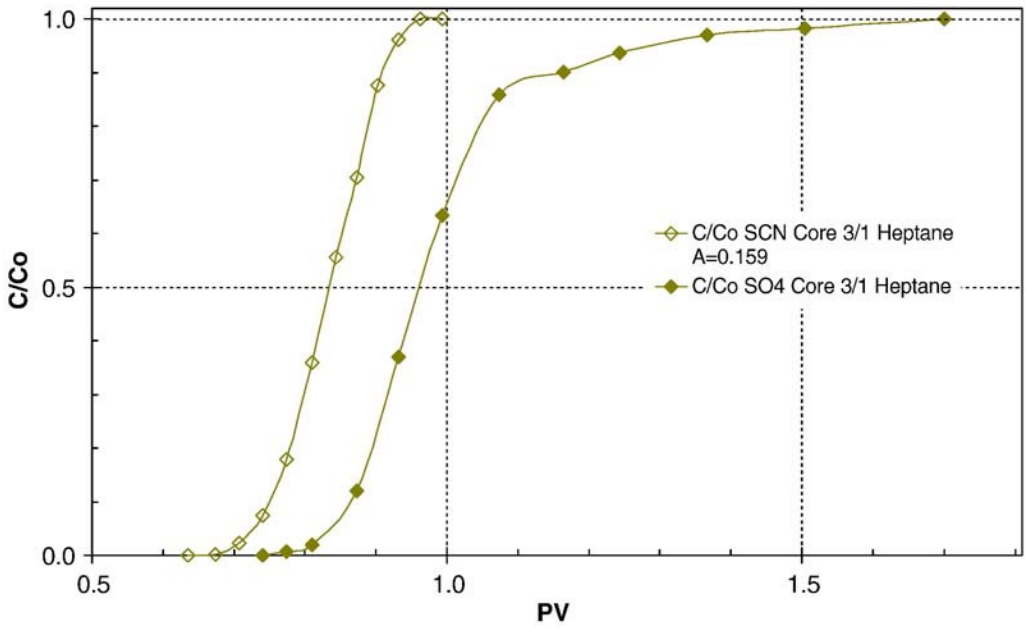

Figure 10: Illustration of the chromatographic wettability test separation between SO_4^{2-} and SCN^- (Strand et al., 2006).

4 Water based EOR in Carbonates

4.1 EOR by smart water in carbonates

Unfavorable wetting properties and the heterogeneous characteristics of carbonate reservoirs makes EOR in these types of reservoirs challenging. Injection of chemicals such as polymers or surfactants is both expensive and represents potential hazard for the environment. As already mentioned, seawater is a smart water for carbonates and has been injected with great success into the Ekofisk field since the 1980`s. It is favorable both from the economical and the environmental point of view. The idea of smart water is to modify wetting conditions by injecting a fluid with optimized composition. The goal is to change the equilibrium of the initial CBR-system, and as a consequence, alter the wettability towards a more water-wet system. This will give increased recovery, as shown in a example Figure 11, where a limestone core is flooded first with formation water (FW) and then seawater (SW). Seawater or modified seawater is often used as the smart water in carbonates, and has especially good effect at higher temperatures.

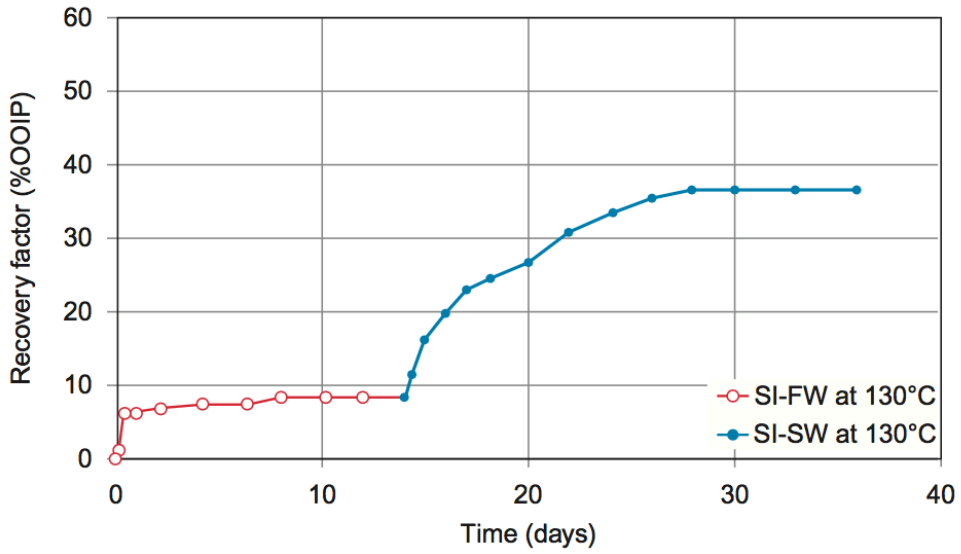

Figure 11: Spontaneous imbibition of formation water (FW), and seawater (SW) into a reservoir limestone core at 130 °C (Ravari, 2011).

4.1.1 Smart water mechanism

The mechanism for the wettability alteration by smart water is suggested to be an interaction between the potential determining ions Ca^{2+}, Mg^{2+}, SO_4^{2-}, the rock surface and the adsorbed oil components (Zhang et al., 2007). All of these ions are present in seawater. Through systematic experimental studies, it has been verified that interaction between these ions at the chalk surface will displace adsorbed carboxylic acids, and hence alter the wettability during smart water injection (Fathi et al., 2010; Zhang et al., 2007). In the formation brine, the content of SO_4^{2-} is usually so low that it is negligible. However in seawater, the concentration of SO_4^{2-} is approximately the double of the Ca^{2+} concentration. The mechanism involves mutual interactions at the chalk surface between Ca^{2+} and SO_4^{2-}, and also between Mg^{2+} and SO_4^{2-}. As a consequence of this, displacement of adsorbed organic materials follows.

Figure 12 illustrates the suggested mechanism for wettability alteration in chalk and limestone by smart water injection. At higher temperatures Mg^{2+} can substitute Ca^{2+} (Figure 12b). If $Mg^{2+}$is able to displace Ca^{2+} from the chalk surface, it must also be able to displace Ca^{2+} connected to the carboxylic groups on the chalk surface (Zhang et al., 2007).

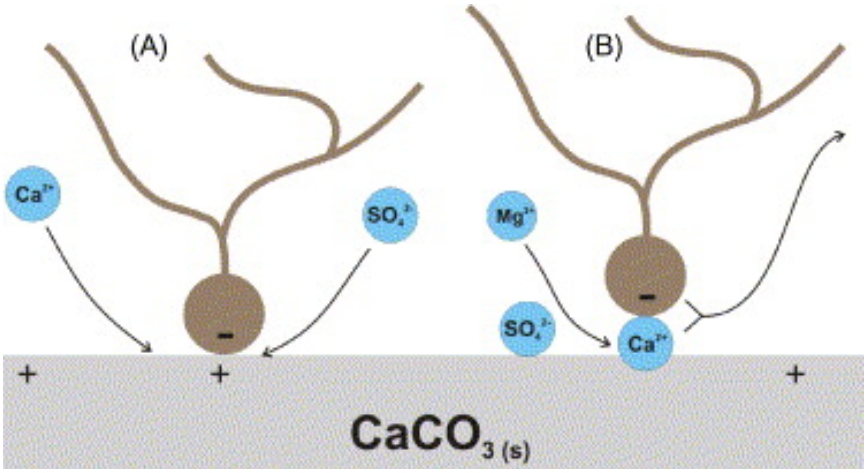

Figure 12: Schematic model of the mechanism of smart water by seawater. (A): Mechanism when Ca^{2+} and SO_4^{2-} are active at lower and higher temperatures. (B): Mechanism when Mg^{2+} and SO_4^{2-} are active at higher temperatures (Zhang et al., 2007).

SO_4^{2-} has also been shown to adsorb more strongly onto the positively charged chalk surface as temperature increases (Rezaeidoust et al., 2009). Spontaneous imbibition studies on chalk cores at 100 °C with various SO_4^{2-} content in the imbibing fluid showed that the seawater with the highest SO_4^{2-} concentration gave the highest recovery (Zhang, 2006). This is shown in Figure 13.

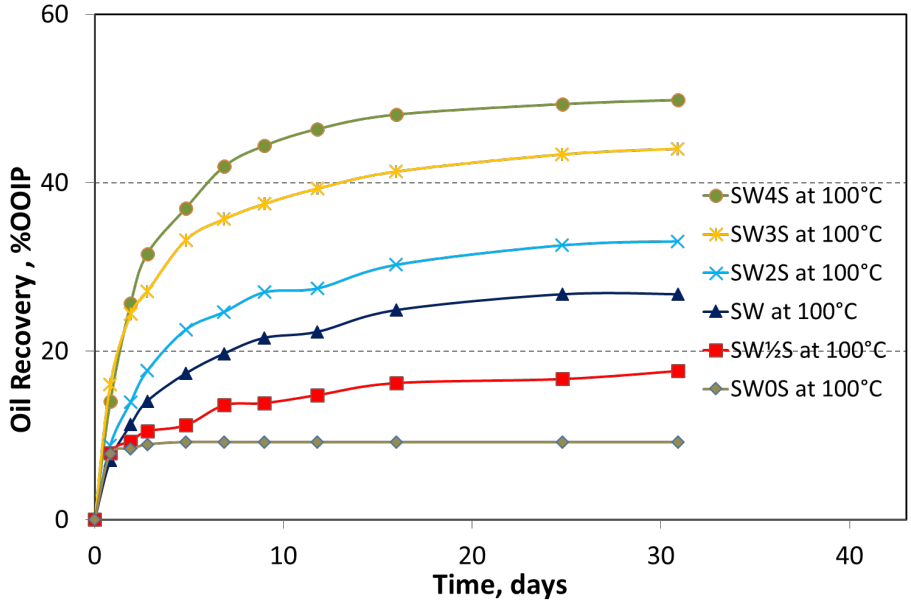

Figure 13: Spontaneous imbibition onto chalk cores at 100 °C, with different SO_4^{2-} content in the imbibing brines (Zhang, 2006).

In the same way, spontaneous imbibition of seawater with increasing Ca^{2+} concentration was studied on chalk cores at 70 °C. The results presented in Figure 14 show that also a high content of Ca^{2+} is desirable for the imbibing brine, giving higher oil recovery.

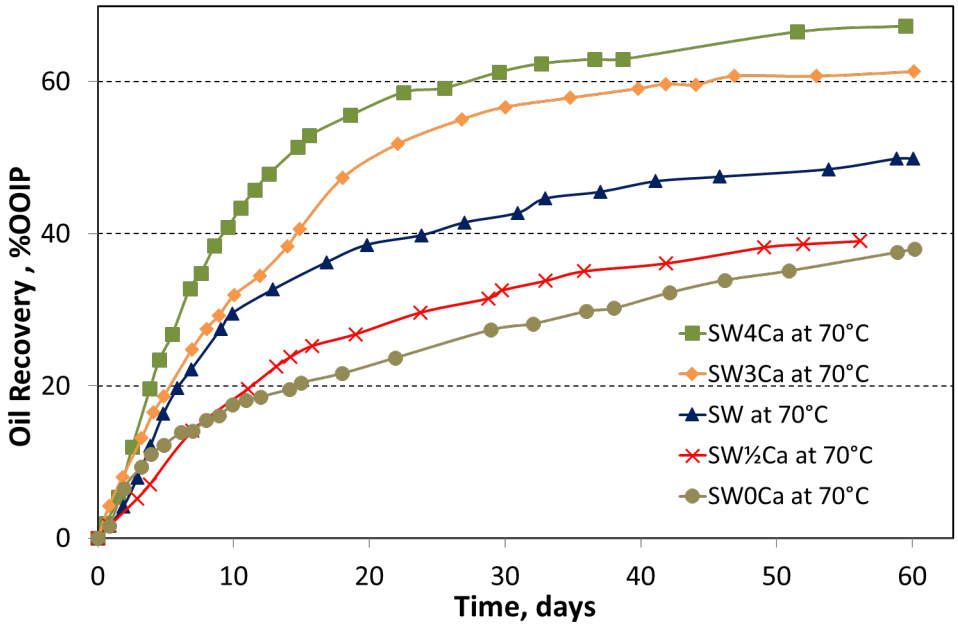

Figure 14: Spontaneous imbibition onto chalk cores at 70 °C, with different Ca^{2+} content in the imbibing brines (Zhang, 2006).

When the SO_4^{2-} adsorbs onto the water-wet sites on the chalk surface it lowers the positive surface charge. As a result of electrostatic repulsion SO_4^{2-} can cause problems with scaling of anhydrite ($CaSO_4$). As already mentioned, the temperature is also of importance in a smart water process.

Further, one can optimize the seawater for EOR injection by changing the composition. Seawater contains Na^+ and Cl^- ions that are not active in the wettability alteration. When removing these ions from seawater, the relative concentrations of the active ions will increase. This will enhance the recovery, compared to injection of seawater with normal composition. Spontaneous imbibition was performed on chalk cores at 90 ˚C, as illustrated in Figure 15. The core was first imbibed with formation brine VB0S, which gave a recovery about 17%. This indicated the core was mixed-wet,. When using SW as imbibing fluid, the recovery was increased to 38% of OOIP, and further to 47% when depleting the seawater of NaCl (SW0Na). SW0Na was further spiked by sulfate, and this resulted in an even higher recovery of 62% of OOIP (Fathi et al., 2011).

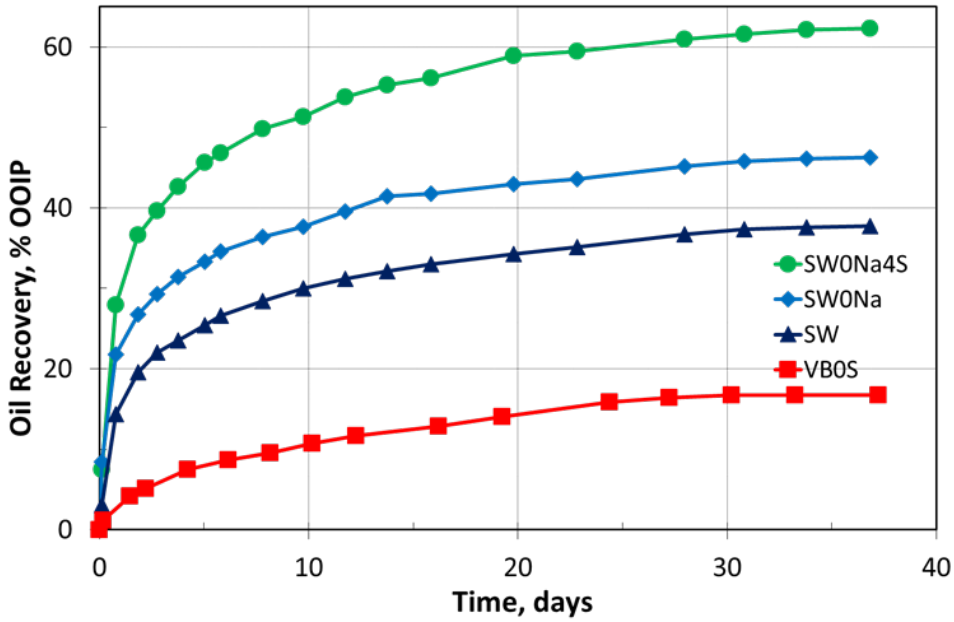

Figure 15: Spontaneous imbibition into oil saturated chalk cores at 90 ºC using VB0S, SW, and modified SW: SW0Na and SW0Na4S (Fathi et al., 2011).

One can thus see that the smart water can be manipulated to become an even smarter water. It should be noted that to be able to utilize a smart water process it is a prerequisite that the system is initially mixed wet. In a completely water-wet system there would be nothing to gain by a smart water flooding. Therefore, the understanding of the initial wettability is of essential importance, and this will further be discussed in the next chapter.

4.2 Initial wetting in carbonates

The initial wetting conditions are, as already mentioned, of crucial importance, especially in the case of naturally fractured reservoirs, where capillary forces are the main driving force for the oil displacement (Shariatpanahi et al., 2011). As deposition and sedimentation take place in an aqueous phase, carbonate reservoirs were originally filled with water. Hydrocarbons later migrated into the reservoir pores and a chemical equilibrium between the crude oil, brine and rock (CBR) was established over geological time (Ahr, 2008; Austad, 2013).

The presence of fractures in a porous, low permeable rock matrix provides a great challenge for producing the oil in reservoir rock. The permeability in the fractures is often several times higher than the permeability of the matrix, and hence the flow from the injector to the producer will mainly pass through the fractures and bypass most of the oil that is mainly outside the fractures. Secondary waterfloods will therefore be less effective. In fractured and low permeable carbonate reservoirs, spontaneous imbibition is the main drive mechanism to obtain a high recovery. In a water-wet rock, the water will imbibe spontaneously into the matrix and expel the oil to the fractures. The challenge is that spontaneous imbibition is most efficient in water-wet rocks, whereas carbonates are mostly neutral to oil-wet. The wetting state prevents spontaneous imbibition of water due to negative capillary pressure. Thus, it would be favorable to increase the capillary pressure through a wettability alteration of the rock surfaces towards a less oil-wet state (Puntervold, 2008; Strand, 2005).

Alteration of a reservoirs rock´s wetting properties may result in enhanced oil recovery. It is therefore essential to understand the mechanisms and factors that affect the wettability. Alterations in wettability have been shown to affect electrical properties, waterflood behavior, capillary pressure, relative permeability and dispersion (Anderson, 1986b). It is also important to differentiate the wettability of sandstones and carbonates. The pH in sandstones is usually low, and hence basic components are attracted easily to the rock surfaces. On contrary, calcite surfaces in carbonates are positively charged and have a higher pH, thus negatively charged ions (acidic oil components) can adsorb on the surface (Abdallah et al., 2007).

4.2.1 Wettability alteration by crude oil

Crude oil is a complex mixture of hydrocarbons and non-hydrocarbon substances. When it comes to wettability, the carboxylic material in crude oil is the most important wetting parameter for carbonate CBR-systemts (Austad, 2013). Crude oil components containing the carboxylic group R-COOH, are mainly found in the crude oil components asphaltenes and resins (Austad, 2013; Buckley et al., 1998). Asphaltenes are the constituents of crude oil with the highest molecular weight. The molecular weight ranges from a few hundred to millions of grams per mole (Speight, 2004). Resins are smaller molecules than asphaltenes, but are in general more polar than asphaltenes due to the relative higher content of the polar elements nitrogen, sulfur and oxygen (NSO compounds). These compounds contain both a polar and a hydrocarbon end, and they adsorb with the polar end onto the rock surface. The hydrocarbon end is oriented outwards, and thus makes the surface oil-wet (Anderson, 1986a; Madsen & Lind, 1998; Puntervold, 2008; Speight, 2014). For carbonates with pH below 8, the surface is positively charged (Pierre et al., 1990). Hence it is the negatively charged carboxylic group in alkaline conditions ($R\text{-}COO^-$) that can adsorb to the carbonate surface. This is illustrated in Figure 16. The bond is very strong, and large molecules will cover the carbonate surface (Austad, 2013). The smaller concentration of the non-active ions Na^+ and Cl^-, the stronger will the adsorption be, as illustrated to the right in the figure.

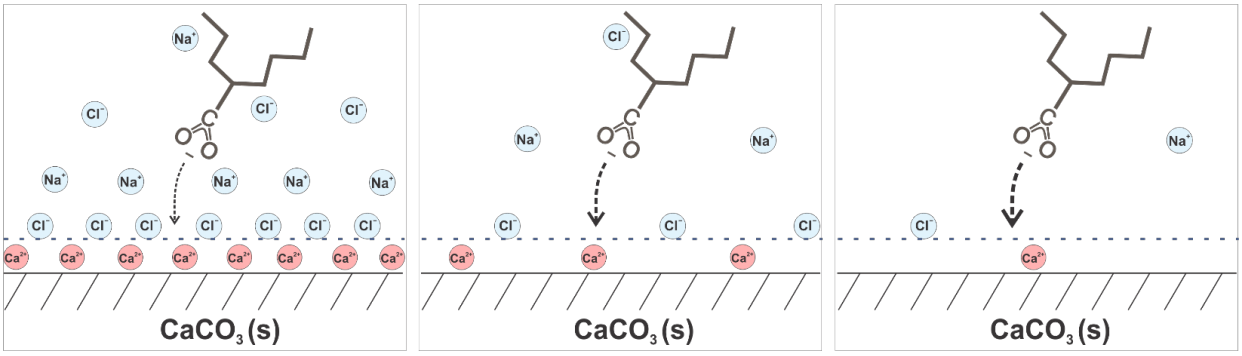

Figure 16: Illustration of adsorption of polar components (Smart water group, 2018).

The polar components will most likely adsorb where the rock surface is directly exposed to the oil-phase. A non-uniform wettability will then occur, where certain areas become covered by an organic layer and become oil wet, while other areas remain water-wet according to the initial wettability (Strand et al., 2006). API-gravity, acid number (AN) and base number (BN) (so called G-AB parameters), in combination with the mineralogy of the rock surface can be

used to evaluate the potential of a particular crude oil to alter the wetting (Buckley et al., 1998)

4.2.2 Effect of initial sulfate

Studies performed by Puntervold et al. (2007a) on Stevns Klint (SK) cores investigated the effect of initial sulfate in cores prior to cleaning. Two cores were studied, and one of them was preflushed with DI water. Spontaneous imbibition was performed on both cores at 90 °C, and the results in Figure 17 clearly show the effect of initial sulfate. The difference in recovery between the two cores was 30%. The non-cleaned core was clearly more water-wet than the cleaned core, due to initial sulfate in the SK cores. The sulfate in the non-cleaned core was involved in the smart water mechanism as described in section 4.1.1. This showed that small deviations in the initial content of sulfate can result in considerable differences in wetting properties. It was concluded that all cores should be flooded with a minimum of 4 PV of DI water to remove soluble sulfate salts from the core.

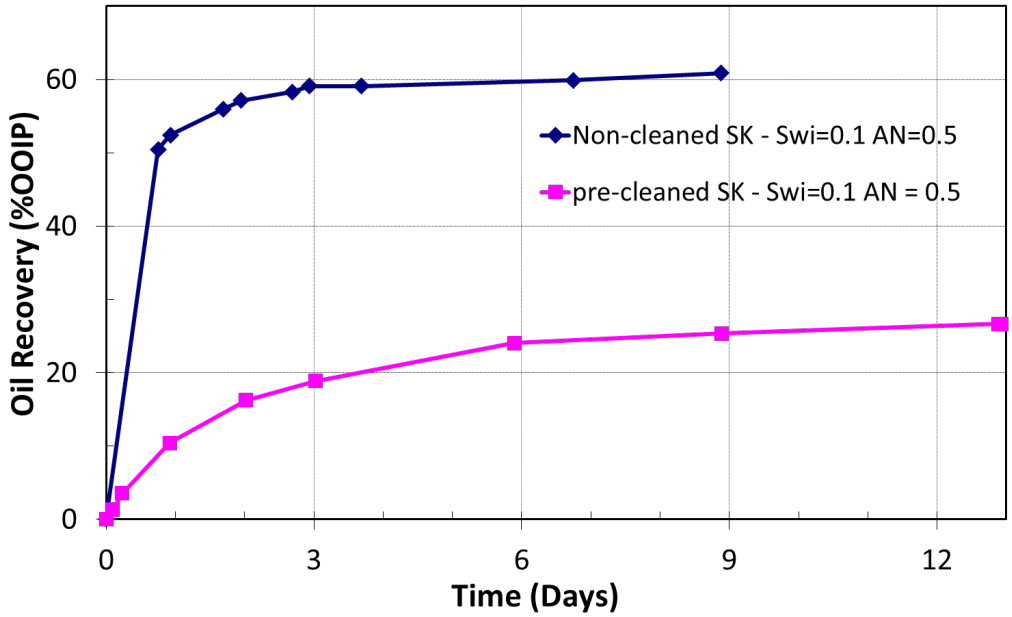

Figure 17: Spontaneous imbibition at 90 °C into non-flushed and flushed SK cores (Puntervold et al., 2007a).

4.2.3 Effect of formation brine composition

Also the composition of the formation brine has shown to have some influence on the initial wetting. Shariatpanahi et al. (2016) found that Mg^{2+} present in the formation brine gave a more water-wet system. Other than that, no significant effects of ion was observed. Using DI-water as initial brine actually gave the least water-wet system. This is illustrated in Figure 18.

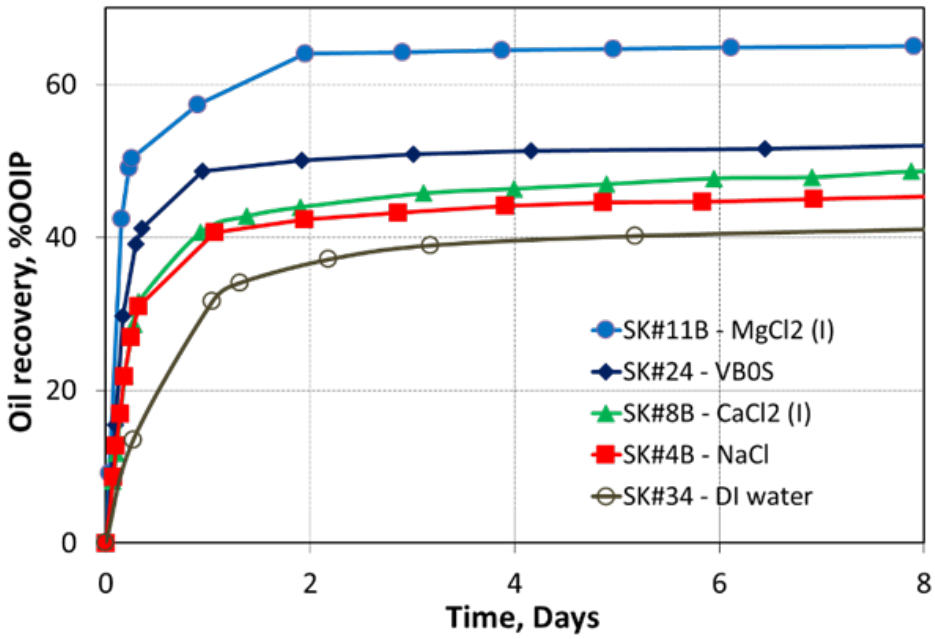

Figure 18: Spontaneous imbibition at 25 °C from SK chalk cores with S_{wi}=0.10 using formation brines with equal salinity, 63 000 ppm, but different type of cations (Shariatpanahi et al., 2016).

The lower wettability by DI water was explained by the lack of ionic double layers outside the chalk surface, something that most likely make it easier for the carboxylic groups to break the water film and adsorb to the chalk surface (Shariatpanahi et al., 2016).

4.2.4 Adsorption of organic acids and bases

Crude oils contain both acidic and basic components. These can be quantified by the acid number (AN) and base number (BN). The AN is the amount in mg of potassium hydroxide (KOH) required to neutralize acid groups in 1 gram of crude oil (mgKOH/g). The number gives a measure of the content of carboxylic acid groups in crude oil, which as already mentioned, is an important parameter for wetting properties. The BN is equivalently the amount in mg of KOH the acids need to neutralize basic material in 1 gram of crude oil (Strand et al., 2016). The numbers can be measured and quantified by potentiometric titration (Fan & Buckley, 2007). Standnes and Austad (2000) studied the effect of various AN on chalk cores. The experimental work showed that as the AN of various crude oils increases, the water wetness decreases. Results from this experiment are shown in Figure 19, where one can clearly see this trend. The crude oil with the lowest AN has a very high oil recovery, whereas the crude oil with the highest AN content almost didn´t have any recovery at all. This confirms that especially the carboxylic material in crude oil has a great impact on the wetting conditions for carbonates. These results were also confirmed by another study performed by Zhang and Austad (2005).

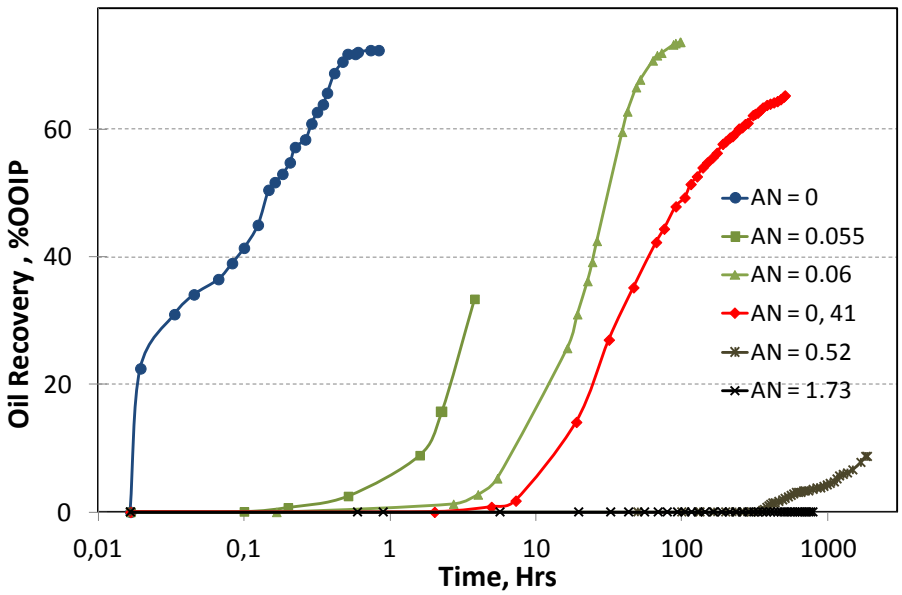

Figure 19: Spontaneous imbibition of brine into chalk cores saturated with crude oils with various AN. The experiments were performed at 50 °C (Standnes & Austad, 2000).

Most of basic components in the crude oil contain nitrogen as a part of aromatic molecules; R_3N: (Strand et al., 2016). Compared to carboxylic acids, the bases seem to have less influence on the initial wettability. However, basic material are able to impact the wettability in some way (Puntervold et al., 2007b). Experiments performed by Puntervold et al. (2007b) studied the impact of basic components on the wetting properties of chalk by using an oil with a constant AN, and varying the AN/BN ratio. For natural bases present in the crude oil, the water wetness increased as the amount of bases increased as shown in Figure 20. This was explained by the formation of acid-base complexes that will prevent some of the carboxylic material to adsorb onto the surface. The core therefore became more water-wet.

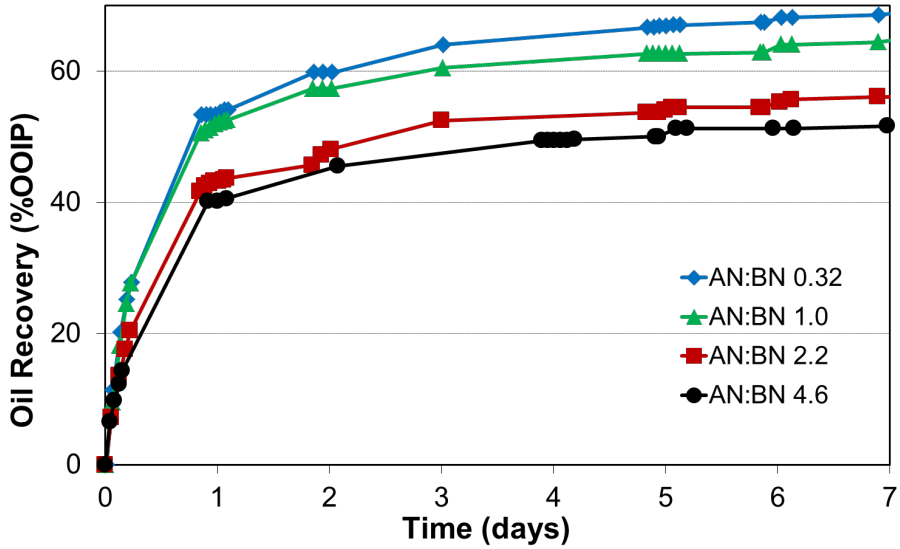

Figure 20: Spontaneous imbibition of oils with constant AN, and various AN/BN ratios from 0.32-4.6 (Puntervold et al., 2007b).

Indirectly, the temperature can also influence the initial wetting (Zhang & Austad, 2005). Studies have shown that over geological time, decarboxylation of carboxylic material takes place at elevated temperatures. $CaCO_3$ could also catalyze this process. This means that the amount of acidic material found in crude oil will be different from the amount that was present when the oil first invaded the carbonate rock (Puntervold et al., 2007b). Basic components seem to have a better tolerance for high temperatures, as the alkaline nitrogen is part of aromatic materials, which are much more resistant to decomposition (Strand et al., 2016). This is the reason why at high temperatures, most crude oils have a higher BN than AN.

4.2.5 Effect of crude oil

Hopkins et al. (2016) studied the adsorption of polar components onto outcrop chalk cores. The result of an oil flooding through an outcrop chalk core not previously exposed to crude oil at 50 °C, is presented in Figure 21. The AN of the effluent was analyzed and plotted against PV flooded. The AN reaches an equilibrium after 10 PVs flooded. The flooding was then stopped for 2 days in order to study the effect of aging where the acidic components are thought to adsorb better. The flooding was then restarted, and no systematic changes in the AN was observed after this period. This indicates that an equilibrium between carboxylic material adsorbed and in the solution has been established. The procedure was repeated at various temperatures, and it was concluded that the temperature had an effect on the time it took to establish adsorption equilibrium. The time it took to obtain adsorption equilibrium of acidic material on the chalk surface decreases as the temperature increased, especially at T > 100 °C. For tests at both 50 °C as in Figure 21 and, also at 90 °C, the adsorption equilibrium was reached after about 10 PVs flooded. For a test at 130 °C it took 7 PV to reach the equilibrium.

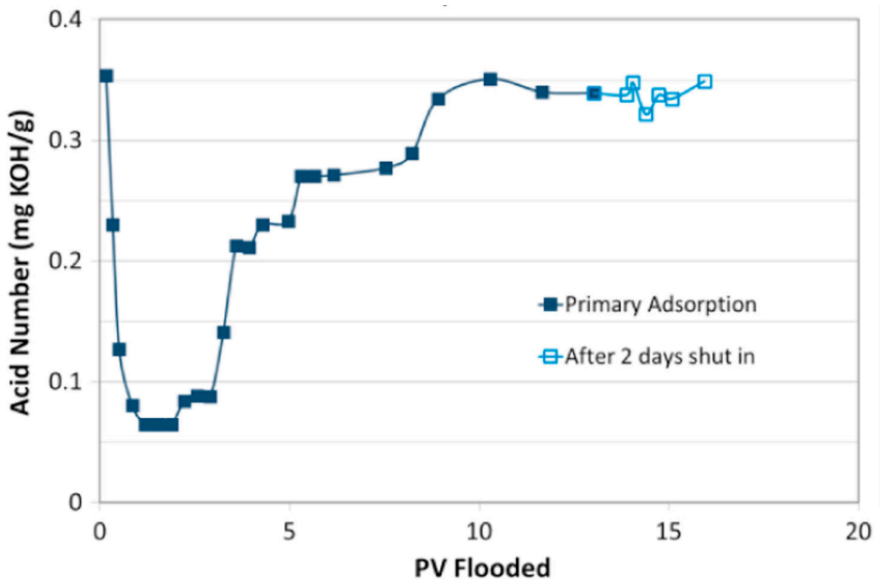

Figure 21: Adsorption of acidic and basic material in terms of AN onto outcrop Stevns Klint chalk cores at 50 °C, using core T1 and oil A with AN=0.34 and BN=0.24 (Hopkins et al., 2016).

An estimation of adsorbing carboxylic groups onto the chalk surface was determined. The total amount of acidic material needed to reach equilibrium (AN_{ads}) is calculated by first estimating the area of a rectangle, that is found by multiplying the AN reference value with the amount of PVs injected to reach this value. From the rectangular area, one then subtract the area under the adsorption curve. The equilibrium value of the AN in oil used in the experiment in Figure 21 was 0.34, i.e $AN_{plateau}$=0.34 mgKOH/g.

$$AN_{ads} = (AN_i)(PV_n) - \sum_{x=0}^{n} \frac{AN_{plateau} - AN_x}{AN_{plateau}} (PV_{x+1} - PV_x) \tag{4.1}$$

The area represents the total amount of acidic organic material adsorbed onto the surface. The area was determined for tests with different crude oils. The results presented in Table 3 show that the adsorbed amount was the same independent of the AN value of the oil. In Figure 22 the same procedure was performed using an oil with the doubled AN as the one used in Figure 21. In this case, the equilibrium was reached after about 8 PVs, and from Table 3 one can see that the adsorption number was similar for all cases at 50 °C. This indicates that the surface has a specific adsorption capacity, independently of the amount of carboxylic material in the oil.

Both the AN and BN was measured. It was observed that also the BN increased during the flooding process, indicating that basic material was also removed by the crude oil. The equilibrium for the basic material was obtained approximately at the same time as the AN equilibrium (Hopkins et al., 2016). A possible explanation for this could be the formation of acid-base complexes between the acidic and basic components, as suggested by Puntervold et al. (2007b).

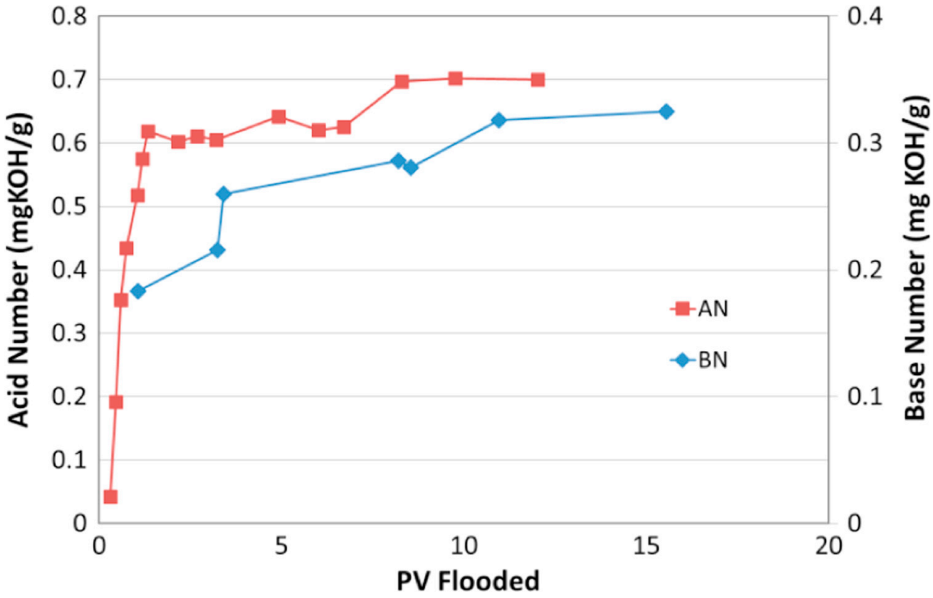

Figure 22: Adsorption of acidic and basic material in terms of AN and BN onto outcrop chalk cores at 50°C using core T5, and oil B with AN=0.69 and BN=0.34 (Hopkins et al., 2016).

Table 3: Summary of results from adsorption of carboxylic groups onto chalk cores and data from wettability tests (Hopkins et al., 2016).

Core – Oil flood. temperature	Adsorption of carboxylic groups	Area from chromatographic wettability test	Water-wet fraction WI
T1-50°C	1.39	0.056	0.17
T4a-50°C	1.47	0.055	0.16
T5-50°C	1.42	n.a.	n.a.

5 Experimental work

In this thesis work the adsorption of basic components in crude oil onto chalk surface, and the wettability alteration by oil flooding is studied. In this chapter, the materials and the methods used in the experiments investigating the adsorption and wettability alteration will be described.

5.1 Materials

In the following sections materials and fluids used in the experiments will be presented.

5.1.1 Safety

All experiments were performed with precaution and by following the HSE-regulations. Several risk assessments were performed to ensure that everyone working in the lab had the knowledge of what to do if something potentially dangerous happened or if something went wrong. Safety measures were taken and security equipment such as lab coat, goggles, gloves, ventilation hoods and masks were used during the experiments.

5.1.2 Core materials

Outcrop chalk samples from Stevns Klint (SK), near Copenhagen, Denmark were utilized as porous media in this study. The Stevns Klint is of Maastrichtian age and is highly porous. The material is similar to some North Sea chalk oil reservoirs; homogeneous and composed mainly of fine-grained, coccolithic matrix. The porosity is approximately 45-50% and the permeability is relatively low, in the range 1-5 mD. A single chalk grain has a general size of 1 μm and has a rather reactive surface area of about 2 m^2/g (Frykman, 2001; Rogen & Fabricius, 2002). The cores were drilled in the same direction and from the same block, by an oversized bit. They were shaved to 3.8 cm in diameter in a lathe, and then cut to a length of 7 cm by a diamond saw.

All tests in this experimental study were performed using two chalk cores with nominally identical properties: core A2 and core A3. Core A2 was tested first, and thereafter core A3 to validate and strengthen the results. Also, a reference core was prepared and tested for comparison of wettability. Properties of the cores utilized in the study are presented in Table 4.

Table 4: Core properties.

Core	A2	A3	Reference
Dry weight, gr	110.2	108.4	110.2
Length, cm	7.04	7.05	7.10
Diameter, cm	3.80	3.81	3.80
Pore volume, ml	38.9	39.7	38.8
Porosity	49%	50%	49%
Initial Water sat.	0.1	0.1	0.1
Permeability (mD)	4.4	3.6	2.0

5.1.3 Oils

For this study an oil with a AN value close to zero and a higher BN value was desirable. It was hence necessary to manipulate crude oils. The model oils were centrifuged for an hour at high rotation speed, and then filtered first with an 8 μm filter, and thereafter with a 5 μm filter. Oil properties are given in Table 5.

Heidrun

The biodegraded Heidrun crude oil with AN=2.80 and BN=0.74 mgKOH/g oil was used as one of the base crude oils. This oil was sampled from a real well during a well test.

RES40

The RES40 oil was prepared by diluting Heidrun oil with n-heptane with a ratio 60:40. The acid and base numbers were measured to AN=1.93 and BN=0.84 mgKOH/g. The dilution with heptane was performed to reduce oil viscosity and hence required pressure to displace the oil.

RES40-0

This oil was prepared by adding 10 wt% of silica gel to the RES40 oil in two steps, and left for stirring for three days each time. This would add a total of 20 wt% of silica gel. The silica gel was added to remove surface-active components in the oil, mostly the carboxylic acid groups but also the basic material. After stirring the mixture with a magnetic stirrer for 6 days, the mixture was centrifuged to separate oil from the silica gel. The silica gel then settled at the bottom of the centrifuge bottle, and the oil was filtered. The acid and base number were measured to AN=0 and BN=0.1 mgKOH/g.

Total crude oil

Total crude oil is also a real reservoir crude oil. This oil was used as base oil and has acid and base number of AN=0.23 and BN=1.85 mgKOH/g.

Oil A

Finally, 115 ml of Total crude oil and 855 ml of RES40-0 oil were mixed, and Oil A was formed. The goal was that this oil should have a AN of 0 mgKOH/g, and a higher BN. The AN was measured to AN=0.07 and BN=0.32 mgKOH/g. The viscosity was 2.87 at 23 °C and 1.87 at 50 °C.

Table 5: Oil properties.

Oil type	ρ [g/cm^3]	AN [mgKOH/g]	BN [mgKOH/g]
Heidrun	-	2.80	0.84
Total Crude Oil	-	0.23	1.85
RES40	0.8130	0.84	1.93
RES40-0	0.8071	0	0.1
Oil A	0.8126	0.32	0.07

5.1.4 Brines

A number of brines were used throughout the study. The brines were synthetically prepared in the laboratory by dissolving the correct amount of salts in de-ionized (DI) water. Chloride, carbonate and sulfate salts were all first dissolved separately in DI water to avoid precipitations during mixing. Then, all solutions were mixed to one solution and diluted to 1 L. The solution was then left for stirring on a magnetic stirrer for approximately 24 hours, to ensure full dissolution. The brines were at last filtrated using VWR vacuum gas pump with a 0,22 μm filter. Table 6 shows the composition for the various brines. A brief explanation of the brines utilized in the thesis:

- **VB0S:** Synthetic Valhall formation water, i.e. based on the Valhall formation located in the North Sea. The brine does not contain SO_4^{2-}. This brine is used as native water and as imbibing fluid during imbibition for all cores.
- **d10VB0S:** Synthetic Valhall brine diluted 10 times with DI water.
- **SW0T:** Synthetic seawater for first part of the chromatographic wettability test. This brine does not contain any SO_4^{2-} or SCN^-.
- **SW1/2T:** Synthetic seawater for chromatographic wettability test. This brine has equal amounts of SO_4^{2-} and SCN^-, and is used in the secondary seawater flooding after S_{or} is reached with SW0T.

Table 6: Composition and properties of brines used.

Brine	**VB0S**	**SW0T**	**SW1/2T**
Ion	[mmol/l]	[mmol/l]	[mmol/l]
HCO_3^-	9.0	2.0	2.0
Cl^-	1066.0	583.0	538.0
SO_4^{2-}	0.0	0.0	120.0
SCN^-	0.0	0.0	12.0
Mg^{2+}	8.0	45.0	45.0
Ca^{2+}	29.0	13.0	13.0
Na^+	997.0	460.0	427.0
K^+	5.0	10.0	22.0
Li^+	0.0	0.0	12.0
Density 20 °C [g/cm^3]	1.042	1.022	1.021
TDS [g/l]	62.38	33.38	33.38

5.1.5 Chemicals

Silical Gel with the grade 60 used for the removal of all acids from the crude oil, and it was supplied by Riedel-de Haën. The n-heptane used for dilution of crude oils and also for cleaning the lines in flooding set-ups had 98% purity, and was supplied by VWR chemicals. All other chemicals used to prepare the brines and chemical reagents were PA-graded and delivered by either Reidel-de Haën, VWR chemicals or Merck. The chemicals used for AN and BN measurements are presented in Appendix A1 and A2.

5.2 Methods

In the following section the various methods utilized in the experiment are explained.

5.2.1 Core cleaning

The cores were initially placed in a Hassler cell for cleaning, illustrated in Figure 23. The cleaning process is according to the method described by Puntervold et al. (2007a). The process is done to remove easily soluble salts, especially SO_4^{2-}. The cores were flooded with 250ml DI water with a rate of 0.1 ml/min at ambient temperature. A confining pressure of about 20 bars was applied. During the flooding, effluent was tested for sulfate by a batch test using Ba^{2+}, where any easily soluble sulfate would visually produce precipitation of $BaSO_4$. After cleaning the cores were placed in an oven with temperature 90 °C and dried to a constant weight. Equation 5.1 represents the chemical reaction for a batch test.

$$Ba^{2+}\,(aq) + SO_4^{2-}\,(aq) \leftrightarrow BaSO_4\,(s) \tag{5.1}$$

During core cleaning the permeability of the cores was calculated using Darcy´s law, presented in Equation 5.2.

$$k = \frac{q\mu L}{A\Delta P} \tag{5.2}$$

Where

k	permeability [mD]
q	flow rate [m^3/s]
μ	viscosity [Pa·s]
L	length of the core [m]
A	cross sectional area [m^2]
ΔP	pressure drop [Pa]

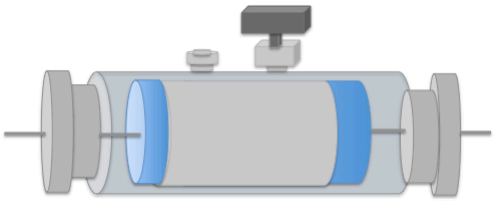

Figure 23: Illustration of a Hassler cell used in the experiments.

5.2.2 Establishing initial water saturation

The dried chalk cores were placed in a desiccator and the gas was removed using a vacuum pump. This is illustrated in Figure 24. The cores were then saturated under vacuum with 10 times diluted formation brine (VB0S). Next, the cores were placed into a desiccator containing silica gel, to vaporize water molecules with silica as an adsorbent. When the weight of the cores corresponded to 10% initial water saturation (S_{wi}=10%) of VB0S, the cores were stored in a sealed container and equilibrated for 3 days to reach an even ion distribution. The procedure is according to the one described by Springer et al. (2003).

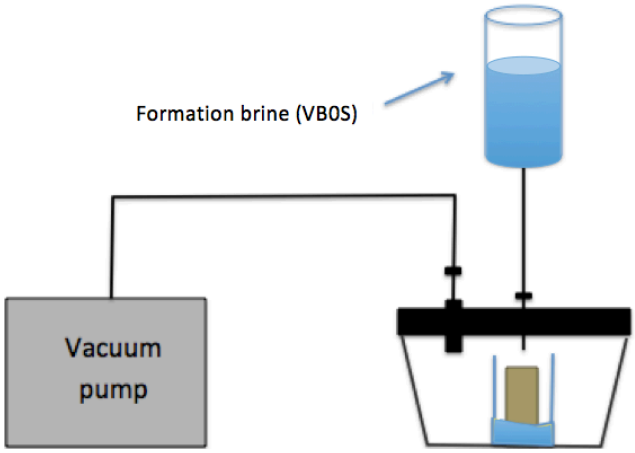

Figure 24: Vacuum pump set-up for saturation of core.

5.2.3 Adsorption of polar components by oil flooding

The chalk cores were placed in a protective rubber sleeve and mounted into a Hassler core holder inside a heating chamber, as illustrated in Figure 25 The cores where then flooded with oil A. During oil flooding confining pressure was set to 7 bars, while the backpressure was 20 bars. The cores were flooded for 4 PV at a constant rate of 0.01 ml/min, and the temperature was 50 °C. Effluent samples of produced oil were collected using an Gilson GX-271 auto-sampler, and the volume of produced oil was calculated based on oil density and produced oil weight. The AN and BN of the oil samples were analyzed by potentiometric titration.

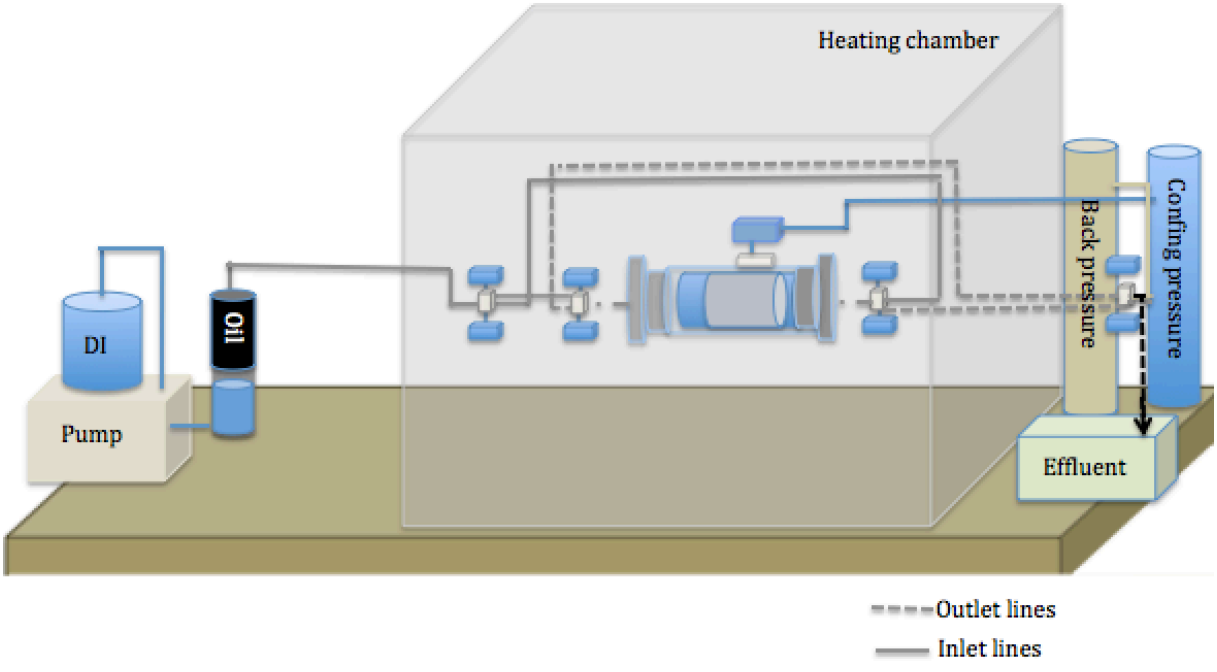

Figure 25: Illustration of oil flooding set-up.

5.2.4 Ageing

Following the oil flooding, the cores were aged. They were wrapped with Teflon tape to avoid unrepresentative adsorption of polar components at the surface, and then placed into a sealed ageing cell surrounded by the same crude oil, and aged for two weeks at 50 °C.

5.2.5 Oil recovery by spontaneous imbibition

The aged cores were evaluated by spontaneous imbibition. The aged cores were immersed in formation water (VB0S) inside a steel imbibition cell, with a piston cell providing 10 bars pressure support. The steel imbibition cell was placed into a heating chamber at 50 °C. A schematic of the setup can be seen in Figure 26. During the imbibition of formation water, no chemically induced wettability alteration was expected to take place. The produced oil as collected in a burette from which the oil level could be recorded directly. The oil recovery was recorded as percentage of OOIP (original oil in place) versus time.

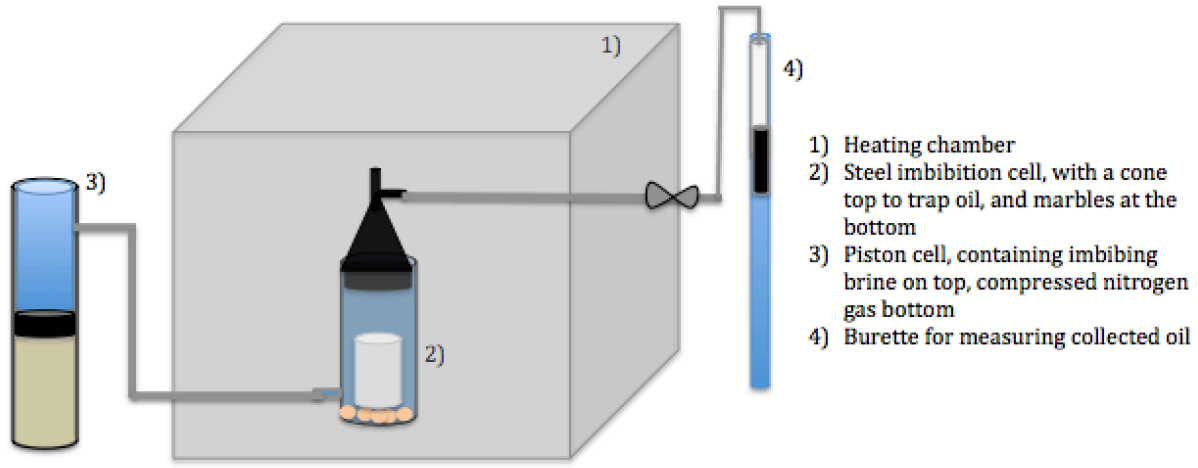

Figure 26: Schematic of spontaneous imbibition procedure.

5.2.6 Oil recovery by forced imbibition

Following the spontaneous imbibition test, the cores were placed into a Hassler core holder. The overburden pressure was set to 20 bars and the back-pressure to 7 bars. Formation brine (VB0S) was flooded through the core at the rate 1 PV/day at 50 °C. Forced imbibition experiments are similar to spontaneous imbibition. The difference is that the water is now pushed through the cores, forcing displacement of oil. Produced oil was collected in a burette and oil recovery (% of OOIP) was reported versus time. When the production had reached a plateau, the flow rate was increased to 4 PV/day to force out any extra oil left. The injection rates are presented in Table 7.

Table 7: PV of cores and injection rates during forced imbibition.

Core	PV	1 PV/day	4 PV/day
A2	38.9 ml	0.027 ml/min	0.108 ml/mn
K8	39.7 ml	0.028 ml/min	0.112 ml/min

5.2.7 Chromatographic wettability test

Chromatographic wettability test was performed after the forced imbibition. This test determines the water-wet area inside a carbonate core based on the measured separation of a non-adsorbing tracer and sulfate, as described in section 3.2.5. After finishing the forced imbibition, temperature was turned off and hence the test was performed at ambient temperature. The cores were flooded with SW0T (containing neither tracer or sulfate) at 0.3 ml/min for 4 PVs to reach S_{or}. Finally, before the main step, a batch test was preformed to ensure there was no SO_4^{2-} in the core. The core was then flooded for 1 more PV at 0.2 ml/min with SW0T, before switching over to SW1/2T, a seawater containing the equal amount of tracer and sulfate. The effluent was collected by an auto-sampler, and areas were determined by ion chromatography analysis of the ion concentration. The results were compared to a 100% water-wet reference core as an indication of core wetting state. The reference core was cleaned in the same manner as the other cores, and a initial water saturation of 10% was established with formation water VB0S. The core was then saturated with heptane and spontaneous imbibition was performed in an Amott cell at ambient temperature. Furthermore, a chromatographic wettability test was performed as a reference.

Area ratios between the thiocyanate and sulfate curves were calculated for all the cores by using trapezoidal method. The WI was also calculated using equation 3.6 in section 3.2.5.

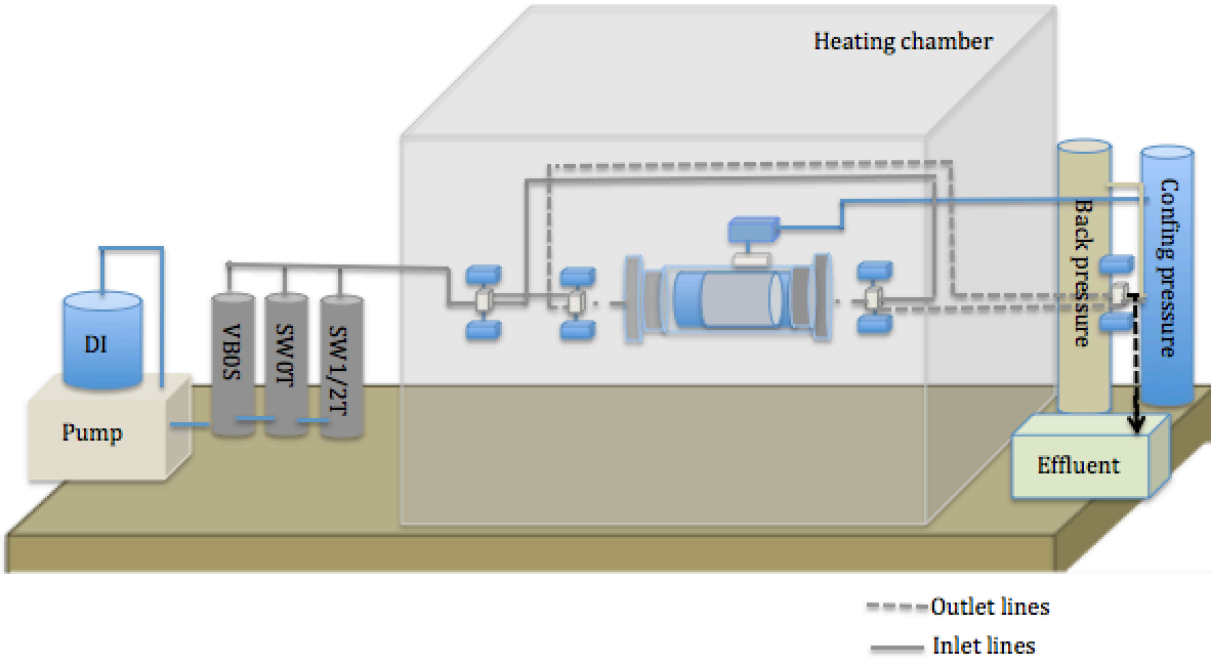

Figure 27: Illustration of the flooding set-up for chromatographic wettability test.

5.3 Analyses

A brief description of the analysis performed as part of the experiments will be presented in the following section.

5.3.1 pH measurements

The pH in the brines was measured using the pH meter seven compact™ from Mettler Toledo. The repeatability of the measurements was ± 0.01 pH units at room temperature, and the electrode used was semi micro-pH.

5.3.2 Density measurements

The densities of the brines and oils were measured using the Anton Parr DMA4500 Density Meter at ambient temperature. Initially the apparatus was cleaned with white spirit, acetone and DI water. Next, a small amount of brine or oil sample was injected into tube and the density was determined. The measurements were repeated to ensure accuracy.

5.3.3 Viscosity measurements

The viscosity of oil was determined using the rotational rheometer Physica MCR 302 from Anton Paar. Approximately 2.2 ml of the oil sample was placed on a metal plate, and then the apparatus was set to measure position with the plates close to each other. The viscosity of the oil was determined through shear stress/shear rate relation.

5.3.4 Determination of AN and BN

The AN and BN measurements of oil samples was done with a Mettler Toledo T55 auto-titrator with an internal standard developed by Fan and Buckley (2007). The standards are modified versions of ASTM D2896 for base number, and ASTM D664 for acid number titration. The instrument uses a blank test as a reference during potentiometric titration of oil samples, where measurement of electronic potential is converted to equivalent acid and base number. Each measurement requires titration solvent and spiking solution, the composition of these can be found in Appendix A.1 and A.2. To secure the test repeatability, a Mettler Toledo weight instruments with accuracy down to the fourth decimal was used. Calibration and blank measurements were made regularly to compensate for changes in electrode properties with time exposed to air. The reproducibility of the measurements was found to be better than ± 0.02 mg KOH/g oil added.

5.3.5 Ion chromatography

Effluent brine samples collected during the chromatographic wettability test were diluted 1000 times with DI water using the trilution™ LH system from a Gilson GX-271 liquid handler. The diluted samplew were further filtered and put into smaller glasses for the analyses. Then, DIONEX ICS-5000^{+} ion chromatograph was used for chemical analyses of both anions and cations. The software controlling the chromatograph uses retention time, which is travel time through the columns. It plots a graph of conductivity versus the retention time where the area under each peak that represents an ion corresponds to their relative concentrations. The ion concentrations of the effluent were calculated based on external standard method.

5.3.6 Scanning electron microscopy (SEM), EDAX

A Zeiss Supra 35VP environmental Scanning electron microscope (SEM) was used to analyze the core structure and size. Small rock samples from the chalk cores were collected to get images of the rock surface. The microscope uses a focused electron beam, which creates an

image by scanning the surface of the sample. Prior to the analysis the samples were prepared with assistance of Emitech K550. They were exposed to vacuum before they were coated with palladium in an argon atmosphere. The preparation was done to prevent erosion of the samples while they were under influence of an electron beam in the SEM (Emitech, 1999).

Elementary analyses of the same rock samples were also taken. The SEM also consists of an EDAX Energy-dispersive X-ray spectrometer (EDS). The core samples used for images were also used for this compositional analyse. Emitted X-rays, from the sample exposed to the electron beam were detected in a Si(Li) detector. The signals were further amplified and presented by voltage (Goldstein, 2003).

5.3.7 Surface area of the cores (BET)

Micromeritics Tristar II, based on the Brunauer-Emmet-Teller (BET) theory, measured the surface area of the SK core. Before the measurement, any adsorbed contamination in the samples was removed by flowing gas, heat and vacuum in a vacuum preparation machine. Micromeritics Tristar II uses nitrogen and helium to calculate the surface area. This was done by measuring the adsorption on the surface of the sample at a specific temperature.

6 Results and discussion

The polar organic components in the crude oil are the key parameters governing the reservoir wettability. The acidic and basic components can adsorb to rock surfaces and act as anchor molecules. In this study the focus has been on the basic components alone, to see if they will adsorb onto the water-wet chalk surfaces or not, and if they will affect the wettability. In order to increase the reliability of the data the experiment was repeated for a second chalk core.

6.1 Core characterization

Small rock samples from the SK chalk cores were collected to get images of the rock surface. Two SEM pictures are presented in Figure 28 and 29. In Figure 28, the picture is magnified 5000 times. One can clearly see some ring structures from the intact coccolithic rings, but mostly fragmented grains. The darker areas between the grains represent the pore system.

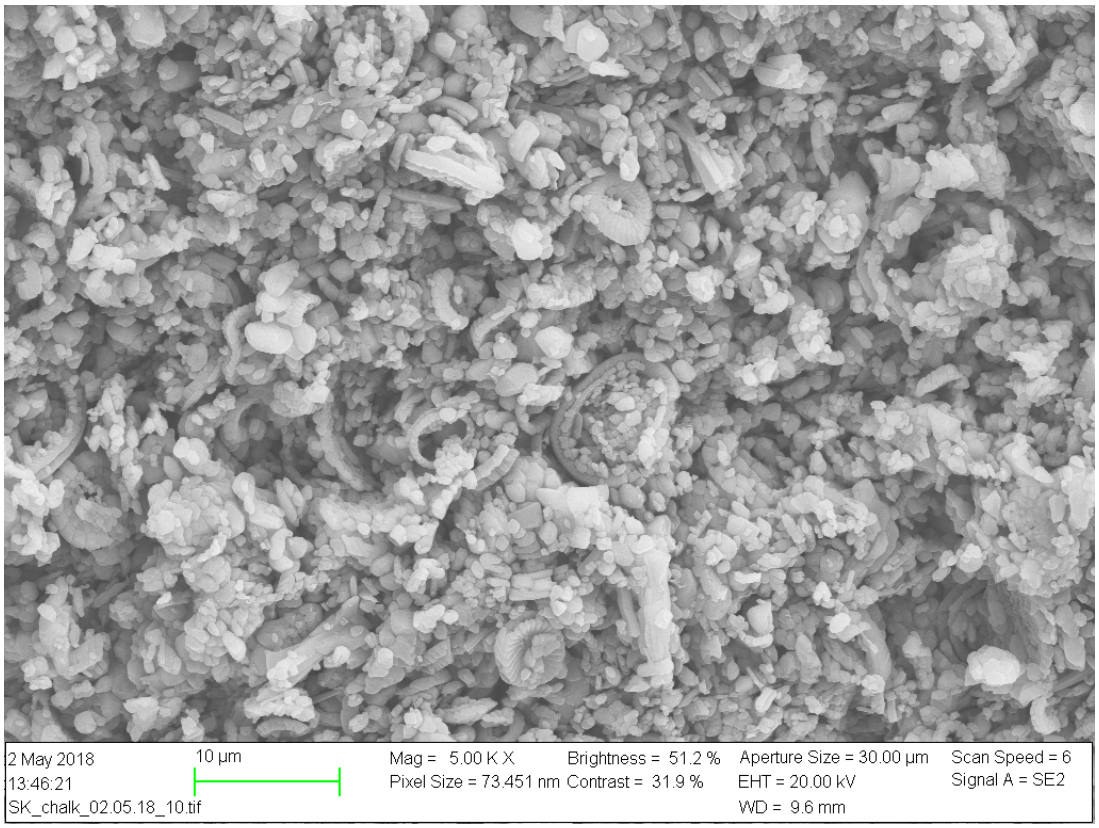

Figure 28: Scanning electron microscopy (SEM) picture of the outcrop SK chalk core, magnification 5000x.

In Figure 29, the magnification is 2000 times, and one can observe that mostly the structure consists of grain fragments with an average particle size of approximately 1 µm. The structure is relatively homogeneous.

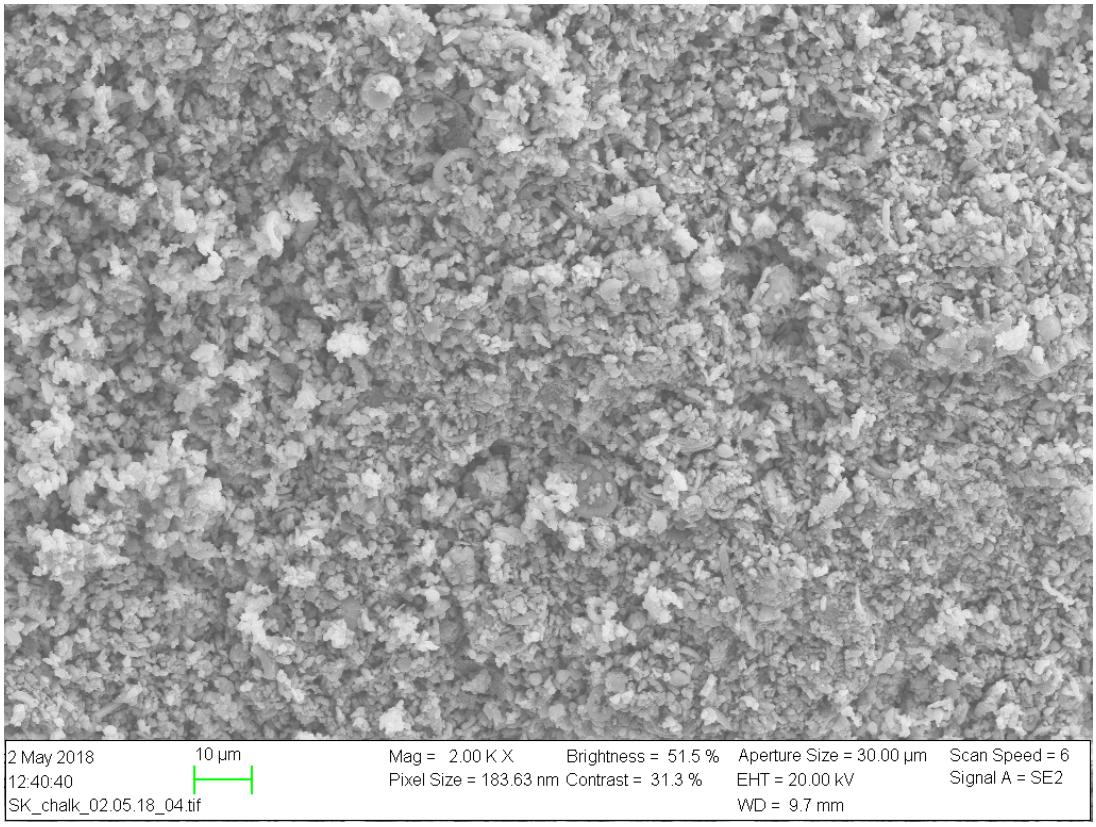

Figure 29: Scanning electron microscopy (SEM) picture of the outcrop SK chalk core, magnification 2000x.

Energy dispersive x-ray spectroscopy (EDS)

Composition analysis of the core was also taken with energy dispersive x-ray spectroscopy (EDS). An average of the values of atomic weight (At %) from two selected areas is presented in Table 8. The values show that we have 99% Ca which indicates a very pure $CaCO_3$. Small values of Mg could be linked to dolomite or $MgCO_3$. Also small values of Al could be linked to clays, but the content is minor. Sulfur (S) could be linked to anhydrite or gypsum ($CaSO_4$ components), but this content is almost negligible.

When cleaning the core for sulfate, a batch test was used to detect sulfate (SO_4^{2-}) as described in section 5.2.1. Sulfate was detected in the early stages of cleaning, but when the batch test was clear and no precipitation was detected one assumed the core was free of S. However, during the composition analysis small amount of S was detected. It could be a possibility that the cores was not completely clean. A better method to detect S during cleaning could have been to analyze the effluent by ion chromatography (IC).

Table 8: Composition analyses by energy dispersive x-ray spectroscopy of SK chalk.

Element	At %
Ca	99.05 ± 0.85
Mg	0.16 ± 0.16
Al	0.11 ± 0.11
S	0.27 ± 0.26

pH analysis

pH analyses of the effluent from the chromatographic wettability test was performed to link the charge of the organic materials. The pH of the SW0T effluent was measured to 7.8, while the SW1/2T was measured to 7.6. Also the VB0S effluent was measured and this had a pH of 7.1. The pH confirms that the environments is slightly alkaline, hence we have dissociated acids and neutral base components as shown by the charge of the organic material at various pH:

Low pH		**Alkaline environment**	
$RCOOH$	$\leftrightarrow$	$RCOO^- + H^+$	(6.1)
R_3NH^+	$\leftrightarrow$	$R_3N + H^+$	(6.2)

At alkaline conditions, the basic components are neutrally charged and it is the negatively charged acidic components that should be active towards the chalk surface.

BET analysis

The BET analysis gave a surface area of 2.1775 m^2/g, which is an expected value for chalk.

Pore size distribution

Milter (1996) studied the pore-size distribution in SK chalk with mercury injection, and his results are presented in Figure 30. The figure shows that most of the pores in this type of chalk have a size in the range of 0.6 μm. The smallest pores have a size diameter just below 0.1 μm, whereas largest pores have a size of 1 μm.

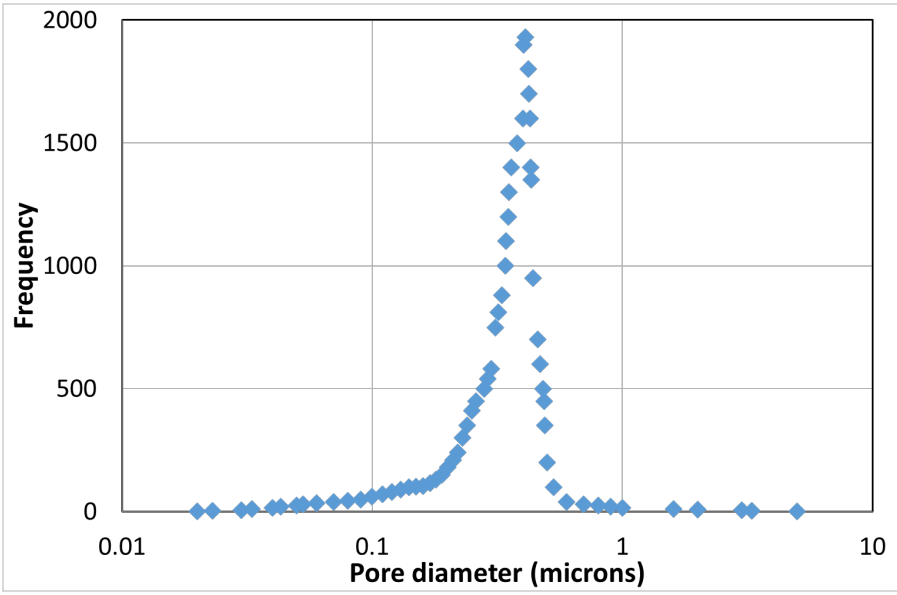

Figure 30: Pore size distribution in Stevns Klint chalk determined by mercury injection capillary pressure curve. Redrawn after (Milter, 1996).

6.2 Water-wet reference core

A reference core was made to compare the results with a 100% water-wet core. The reproducibility of SK chalk in previous wettability and smart water studies has been found to be very good (Hopkins, 2016). The SK behave very water-wet, and this was confirmed by a spontaneous imbibition test on a reference core with S_{wi}=10%, saturated with heptane. VB0S was used as formation water. As one can see in Figure 31, 70% of heptane was produced from the core by strong positive capillary forces within less than one hour. After 15 days 71% of OOIP had been produced.

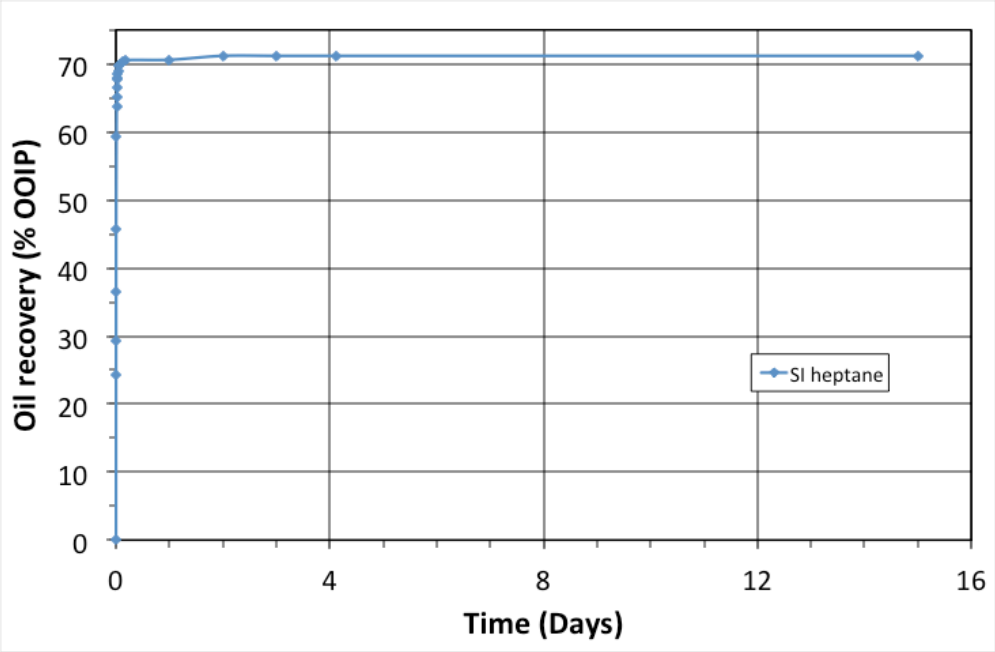

Figure 31: Oil recovery by spontaneous imbibition of formation water on reference core at ambient temperature.

A chromatographic wettability test was also preformed in order to define a measurement of a completely water-wet surface area for SK outcrop chalk. The test was performed at ambient temperature by flooding first with SW0T, followed by SW1/2T brines. As can be seen in Figure 32, the 100% water-wet core had a water-wet surface area of $A_{heptane}$= 0.287. This represents the wettability index (WI) equal to 1.

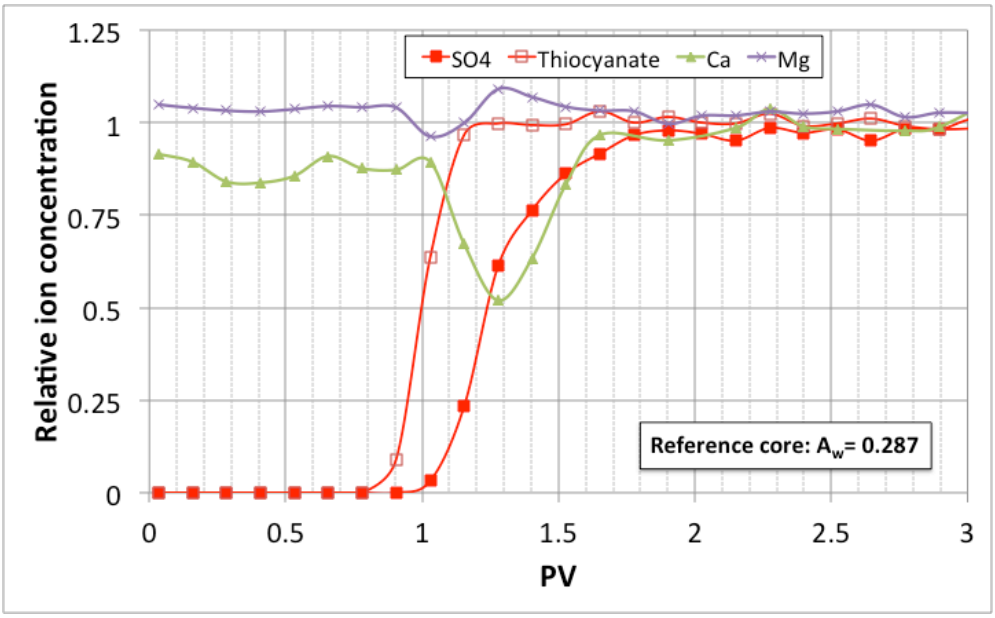

Figure 32: Chromatographic wettability test results performed on a reference core.

6.3 Adsorption of polar components onto water-wet chalk surface

Two chalk cores with initial water saturation of S_{wi}=10% were flooded with 4 PV of crude oil A. The temperature was 50 °C and the flooding rate was 0.1 ml/min. Oil A contained a moderate amount of basic components with BN=0.32, and close to zero of acidic components with AN=0.07. The adsorption of polar components was evaluated by analyzing effluent oil samples.

The base number measurements from the flooding of core A2 are presented in Figure 33. The dashed line presents the BN of the oil measured before flooding as a reference. From the plot one can see that the first BN value is at 0.1 mgKOH/g. The BN values further increases rapidly and reach the reference value already before 2 PVs injected. This indicates a rather small adsorption compared to what Hopkins et al. (2016) found for acids. The absence of any significant adsorption is expected and consistent with the previous findings by Puntervold et al. (2007b).

Hopkins et al. (2016) determined the total amount of acidic organic material adsorbed onto the surface, by using equation 4.1 in section 4.2.5. In the same way, an estimation of adsorbing basic material (BN_{ads}) onto the chalk surface was estimated. The formula was then reformulated to equation 6.3. The base adsorption (BN_{ads}) was defined with the equilibrium value $BN_{plateau}$=0.32 mgKOH/g, and by use of the following equation:

$$BN_{ads} = (BN_i)(PV_n) - \sum_{x=0}^{n} \frac{BN_{plateau} - BN_x}{BN_{plateau}} (PV_{x+1} - PV_x) \qquad (6.3)$$

The area above the adsorption curves represents the total amount of basic organic material adsorbed onto the surface. The area was determined to be BN_{ads}=0.26 for core A2. Comparing

to the values of adsorption of carboxylic groups in Table 3, this is a small value, which is in line with the results so far.

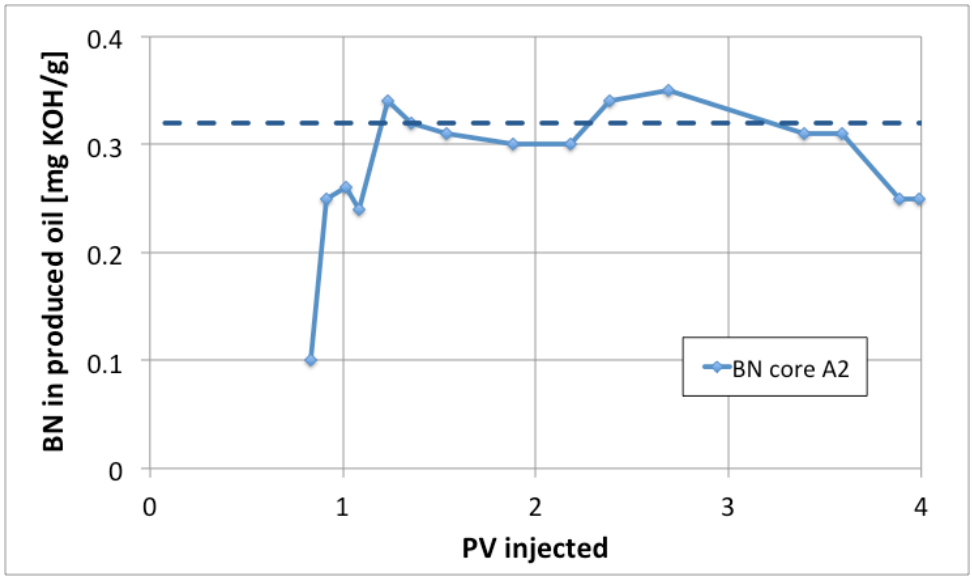

Figure 33: Base number measurements of effluent oil samples collected from oil flooding of core A2.

In Figure 34, the AN from oil flooding of core A2 is also included. The reference AN is presented by the dashed red line at 0.07 mgKOH/g. The values are unstable from 0 to 0.11 mgKOH/g through all the samples. This could be due to the sensitivity of the measurements at such low values. It appears that there is a small adsorption of acids, and formation of acid-base complexes at the chalk surface could be an explanation for the observed adsorption of bases. Due to the uncertainty of the AN measurements, it is hard to conclude whether there is any adsorption of acids or not, and to quantify the potential adsorption.

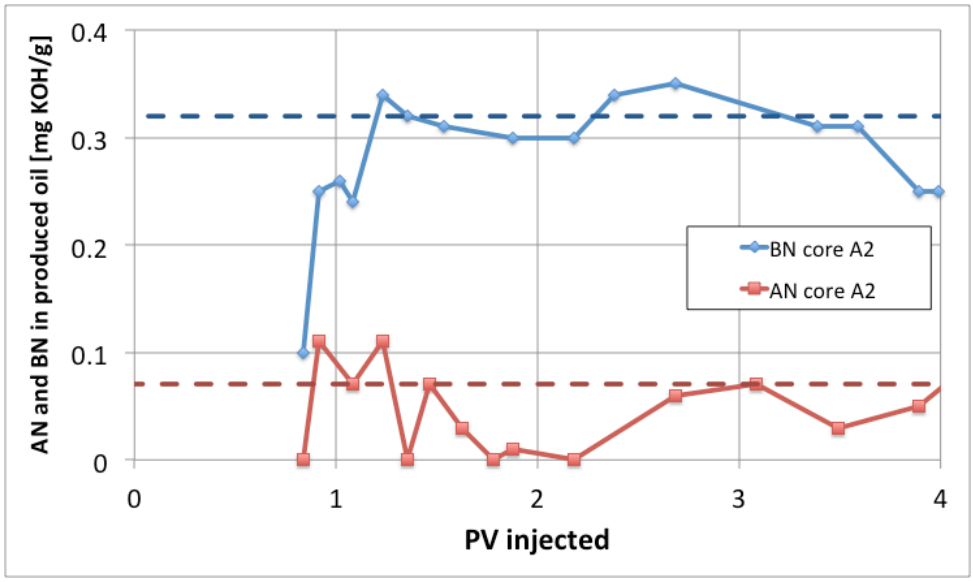

Figure 34: Acid and base number measurements of effluent oil samples collected from oil flooding of core A2.

The second core, A3, was treated in the same way as core A2. In Figure 35, the base number of the produced oil samples is presented. Also these show about 0.1 mgKOH/g for the first effluent sample, followed by a rapid increase to the reference value BN=0.32 mgKOH/g. The BN reaches this value before 2 PVs of oil is injected, and seems to have reached equilibrium at this level. This is in line with the results found from the first core (A2). The adsorbed amount of bases was quantified to BN_{ads}=0.36 for core A3 by using equation 6.3.

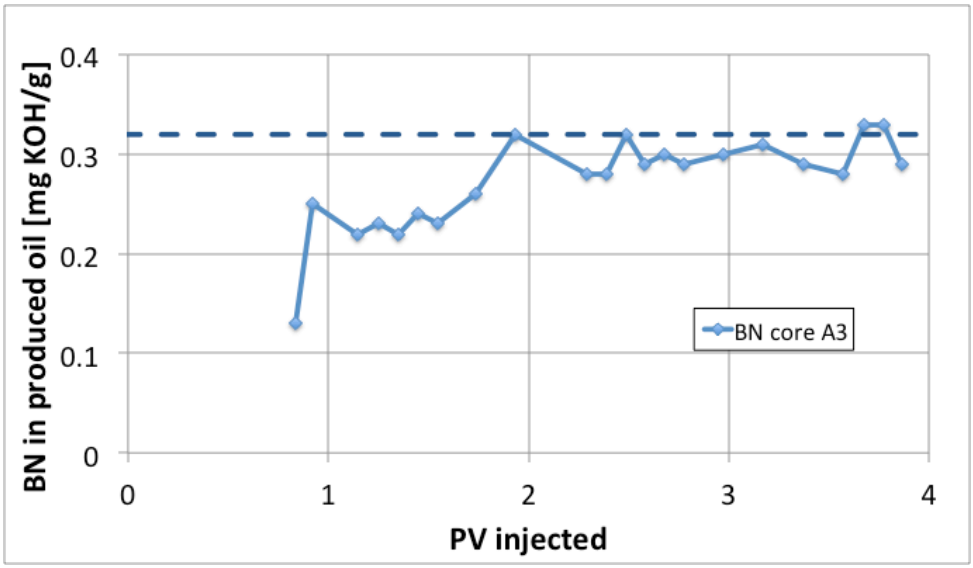

Figure 35: Base number measurements of effluent oil samples collected from oil flooding of core A3.

Figure 36, includes also the AN values of the oil effluents from core A3. Similarly to the case of the A2 core, the values of AN are a bit unstable. This could, as already mentioned, be due to the sensitivity of the instrument at such low values, and makes it difficult to draw a conclusion about the adsorption of acids.

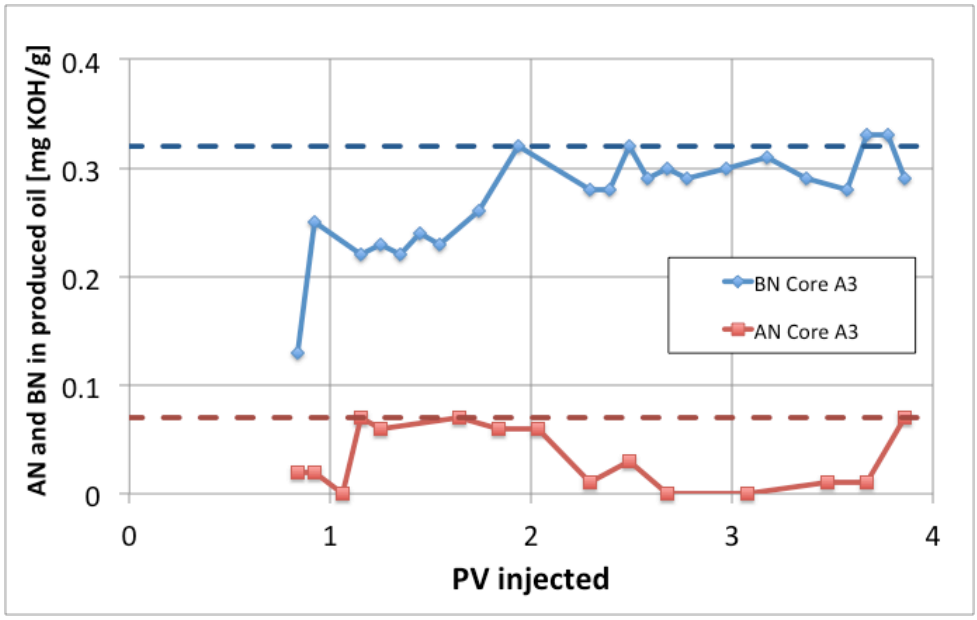

Figure 36: Acid and base number measurements of effluent oil samples collected from oil flooding of core A3.

The two cores give very similar results. A potential adsorption is detected in between the first and second injected PV. After this the equilibrium is reached, and this is quite fast compared to what Hopkins et al. (2016) reported in their work with adsorption, as illustrated in Figure 21 and 22 in section 4.2.5, where the equilibrium was reached typically after 8 or 10 PVs. One can conclude that, in the current study, there is very little adsorption compared to what was seen in the work of Hopkins. The BN_{ads} of 0.26 and 0.36 are also small values compared to the ones reported by Hopkins et al. (2016) determined for adsorption of acidic material. As there were small traces of acidic components in the oil used, the small adsorption that is seen for basic components could be a result of formation of acid-base complexes. The bases are adsorbed together with the acids.

The results can also be compared with the findings reported by Hopkins et al. (2016), presented in Figure 22, section 4.2.5. The oil used had a very similar BN to oil A in the current study, but had a much higher AN; AN= 0.69 and BN=0.34. From Figures 34 and 36 one can hence observe that lowering the AN, also lowered the adsorption of bases even though Oil A in this experiment had almost the exact same BN value as in the study by Hopkins et al. (2016). It indicates that the bases follow the acids, and only adsorb due to connection with AN.

6.4 Oil recovery and wettability

After the flooding of crude oil, the cores were aged for 14 days. Thereafter, spontaneous imbibition of formation water VB0S was performed at 50 °C. When the oil production had reached a plateau, forced imbibition followed in two stages: first at 1 PV/d, and then at 4 PV/d. The results are presented in Figure 37 and 38. In both cases, one can see that the oil recovery is quite high. For core A2 the oil recovery is approximately 53% of OOIP after 11 days. The high recovery and also the piston-like shape of the curve indicate that there are strong capillary forces and that A2 is a quite water-wet core. The forced imbibition that

followed further increased the production to 62% after 14 days. Increasing the injection rate from 1 PV/d to 4 PV/d did not seem to have a noteworthy effect.

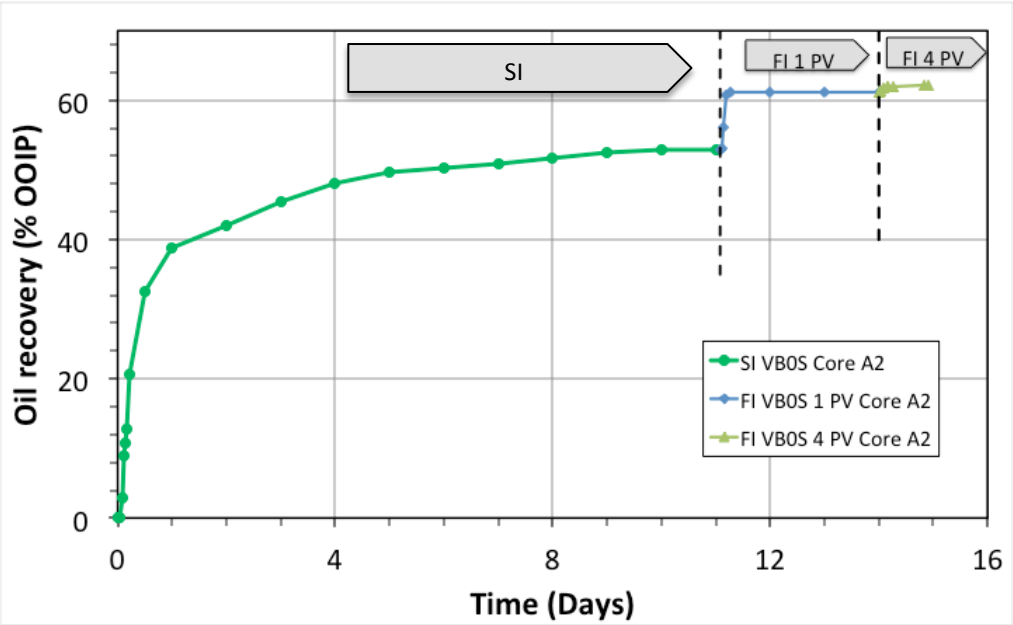

Figure 37: Oil recovery by spontaneous and forced imbibition of formation water on chalk core A2 at 50 °C.

Results for core A3 presented in Figure 38, confirms the results found for core A2. The recovery by spontaneous and forced imbibition was quite similar to that observed from core A2. Spontaneous imbibition for 11 days gave an oil recovery of approximately 53% of OOIP. Forced imbibition increased the recovery to 59% of OOIP after 15 days.

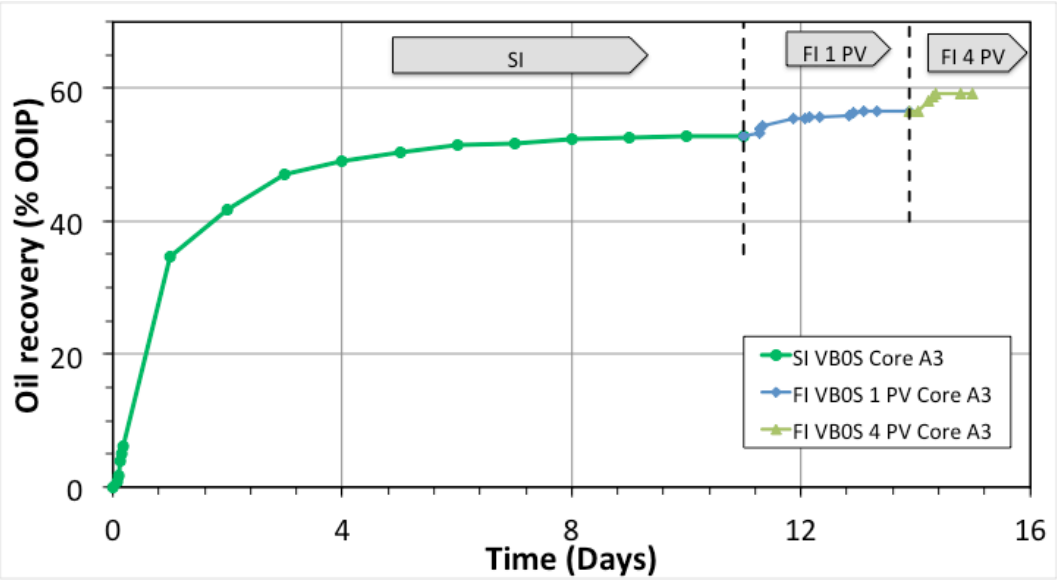

Figure 38: Oil recovery by spontaneous and forced imbibition of formation water on chalk core A3 at 50 °C.

Using equation 3.2 from section 3.2.3, one can determine the "displacement-by-water-ratio", I_W, as calculated in equation 6.4 and 6.5 for core A2 and A3 respectively. Both values are close to 1, and indicate a quite water-wet system.

$$I_{W,A2} = \frac{0.53}{0.53 + 0.09} = 0.85 \tag{6.4}$$

$$I_{W,A3} = \frac{0.53}{0.53 + 0.07} = 0.90 \tag{6.5}$$

In Figure 39, the spontaneous imbibition from the completely wet reference core is compared to the results observed from core A2 and A3, after they had been flooded with oil. It is clear that there has been a change in the wettability of the cores exposed to oil.

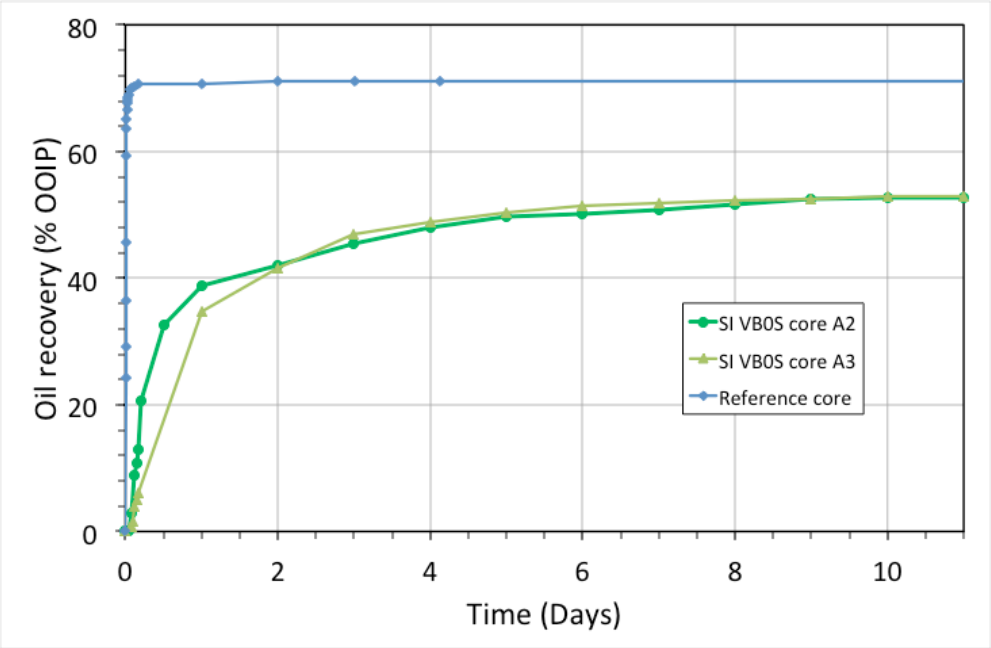

Figure 39: Oil recovery by spontaneous imbibition of formation water on chalk cores A2, A3 (50 °C) and on the reference core (ambient temperature).

The spontaneous and forced imbibition confirms that the wettability of the cores has in some way been affected by the small adsorption observed. In a previous study by Puntervold et al. (2007b) one found that by increasing the amount of basic material in the oil reduced the adsorption of acids, and made the core more water-wet compared to results from oils with lower BN. In this study we see that the oil has affected the wettability to some extent. Most likely this is due to adsorption of acids. The adsorption happens immediately.

6.5 Chromatographic wettability test

Following the spontaneous and forced imbibition, the cores were flooded until S_{or} was established, and then a chromatographic wettability test was performed. The experiment was conducted at 25°C. The results are presented in Figure 40 and 41. As can be seen from the Figure, the area between the SO_4^{2-} and thiocyanate curves for core A2 A_W=0.249 is still relatively large and indicates a quite water-wet system.

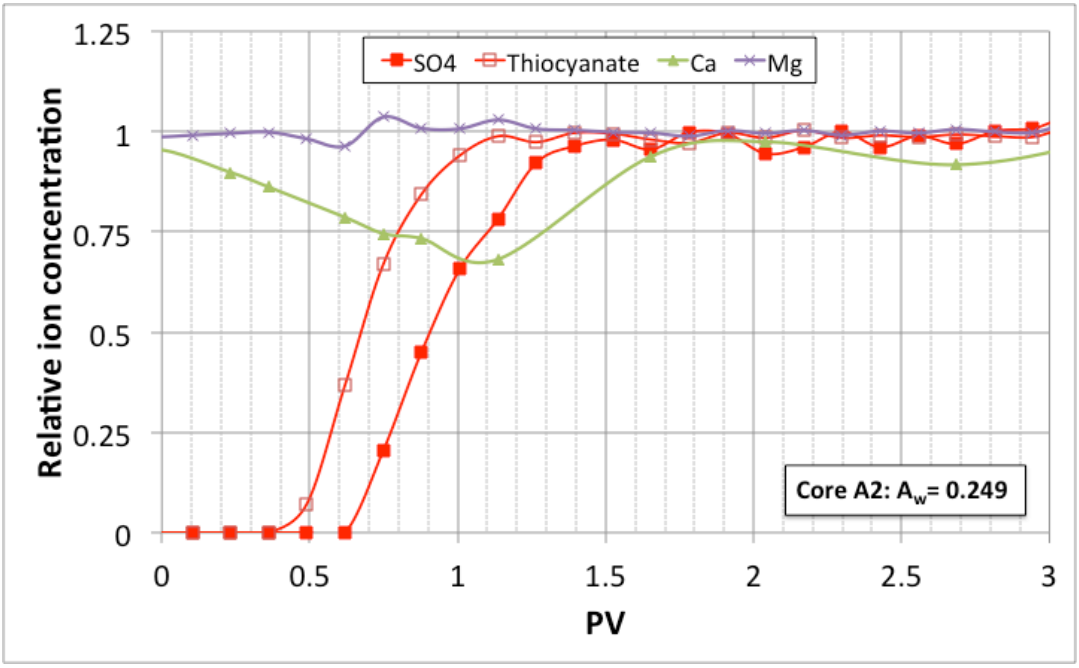

Figure 40: Chromatographic wettability test of core A2, resulting in an area of Aw=0.249.

Using the area from the reference core one can calculate the wettability index as described in section 3.2.5. This gives a WI=0.87, as shown in equation 6.6.

$$WI = \frac{0.249}{0.287} = 0.87 \tag{6.6}$$

The wettability index of 0.87 confirms that the core is quite water-wet, and hence has not been affected much of adsorption.

The results for core A3 is presented in Figure 41, and are similar to the results for core A2. The area is A_W= 0.223 and indicates a quite water-wet system. Calculating the wettability index for core A3 gives:

$$WI = \frac{0.223}{0.287} = 0.77 \tag{6.7}$$

The wettability index of 0.77 again confirms that the core is quite water-wet, and is in line with the results found for core A2.

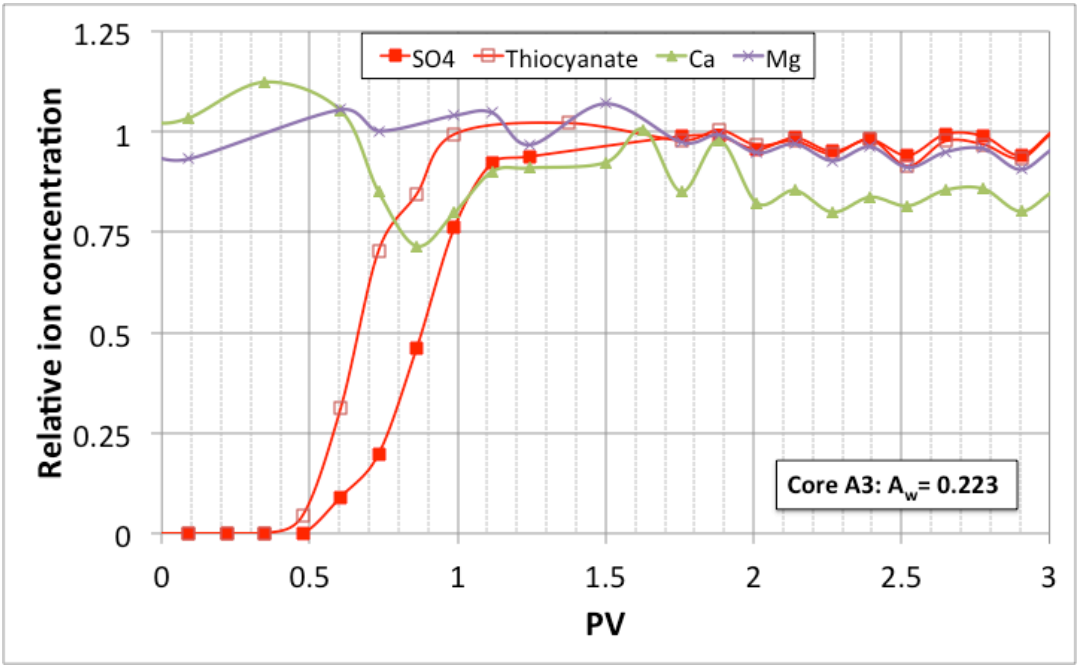

Figure 41: Chromatographic wettability test of core A3, resulting in an area of Aw=0.252.

6.6 Summary

The behavior of basic components on the chalk core surface was studied. The results showed good reproducibility on adsorption testes. The adsorption of bases was low, first value was around 0.1 and increased rapidly to equilibrium. The values for acid number were rather low and fluctuating, and it is difficult to say conclude with certainty, but most likely there was some adsorption of acids as well. The spontaneous and forced imbibition tests performed after oil flooding showed good reproducibility, and that the wettability had not been altered much. This was confirmed by chromatographic wettability test, and one can conclude that the wetting was altered from very water-wet to quite water-wet. The WI for the two cores were 0.87 for core A2 and 0.77 for core A3. Table 9 gives a summary of the results.

Table 9: Summary of the experimental results.

Core	BN_{ads}	Oil recovery by SI [% of OIIP]	Oil recovery by FI 1PV/d [% of OIIP]	Oil recovery by FI 4 PV/d [% of OIIP]	Total recovery by SI and FI [% of OOIP]	WI
Ref-core	-	71	-	-	71	1
A2	0.26	53	8	1	62	0.87
A3	0.36	53	3	3	59	0.77

The adsorption of bases was quantified to BN_{ads}=0.26 and BN_{ads}=0.36. These are small values compared to the adsorption of acids reported by Hopkins et al. (2016), presented in Table 3. In the study by Hopkins et al. (2016) presented in Figure 22, an oil with similar BN, but higher AN than in the current study was used. From the experimental results in the current study it is observed that lowering the AN also lowered the adsorption of bases. This indicates that the basic components follow the acidic components. Based on the results from Puntervold et al. (2007b), where one saw that an increased amount of bases reduced the adsorption of

acids and made the core more water-wet, one can conclude that the small wettability alteration observed in the experiments from very water-wet to quite water-wet is most likely due adsorption of acids. Due to uncertainty in the measurements of the adsorption of acids at such low values, the quantification becomes difficult. Good reproducibility of the results was observed.

Conclusions

The main objective of this thesis was to get a better understanding of how basic components in the crude oil adsorb onto the rock surface. In order to do so, two outcrop chalk cores were flooded with an oil containing much larger amount of bases compared to acids. In the tests performed, a small adsorption of bases was observed, most likely due to formation of acid-base complexes. The experimental observations led to the following conclusions:

- A 100% water-wet reference core prepared with heptane, spontaneously imbibed with FW gave an oil recovery of 71% of original oil in place (OOIP).
- The measured AN lies within the area of uncertainty, but for the BN one can see that there is instantaneous adsorption. The BN values quickly reached the equilibrium value, most likely because the basic material is linked to the acidic components.
- The adsorbed basic material was quantified to BN_{ads}=0.26 and BN_{ads}=0.36. These values are low compared to the AN_{ads} in the studies by (Hopkins et al., 2016).
- Compared to previous work (Hopkins et al., 2016) using oils with close to equal BN, but higher AN, one observed a large decrease of adsorption of bases. This indicates that the bases may complexate the acids.
- Spontaneous imbibition of the cores after crude oil flooding gave oil recovery of 53% of OOIP for both cores. Following forced imbibition gave total recovery of 62% for core A2 and 59% for core A3. This shows that the wettability is still on the water-wet side after oil flooding.
- Chromatographic wettability confirmed that the wettability had changed from very water-wet to quite water-wet, due to a small adsorption.

For future studies it would be convenient to try to further reduce the AN. This would help to differentiate if the instability of the AN values was caused by uncertainties in the detection limit or by method of preparation. One could also repeat the same tests for more cores from the same formation to test the reproducibility further, and once this is confirmed one could test this experiments in other chalk samples with different mineralogy, e.g. Aalborg chalk.

It could also be interesting to observe the effect of wetting by changing the BN, by performing tests with both higher and lower BN, but still maintaining the AN at 0, or at very low values.

References

Abdallah, W., Buckley, J. S., Carnegie, A., Edwards, J., Herold, B., Fordham, E., Graue, A., Habashy, T., Seleznev, N., Signer, C., Hussain, H., Montaron, B., & Ziauddin, M. (2007). Fundamentals of wettability. *Oilfield Review, 19*(2), 44-61.

Abdelgawad, K. Z., & Mahmoud, M. A. (2014). *High-Performance EOR System in Carbonate Reservoirs*. Paper presented at the SPE Saudi Arabia Section Technical Symposium and Exhibition, Al-Khobar, Saudi Arabia.

Ahr, W. M. (2008). *Geology of carbonate reservoirs: the identification, description, and characterization of hydrocarbon reservoirs in carbonate rocks*

Amott, E. (1959). *Observations Relating to the Wettability of Porous Rock*.

Anderson, W. G. (1986a). Wettability Literature Survey- Part 1: Rock/Oil/Brine Interactions and the Effects of Core Handling on Wettability. doi:10.2118/13932-PA

Anderson, W. G. (1986b). Wettability Literature Survey- Part 2: Wettability Measurement. doi:10.2118/13933-PA

Anderson, W. G. (1987). Wettability Literature Survey-Part 6: The Effects of Wettability on Waterflooding. doi:10.2118/16471-PA

Austad, T. (2013). Water-Based EOR in Carbonates and Sandstones: New Chemical Understanding of the EOR Potential Using "Smart Water" *Enhanced oil recovery field case studies* (pp. 301-335): Elsevier Science.

Bavière, M. (Ed.) (1991). *Basic concepts in enhanced oil recovery processes* (Vol. 33). London: Published for SCI by Elsevier Applied Science.

Buckley, J. S., Liu, Y., & Monsterleet, S. (1998). Mechanisms of Wetting Alteration by Crude Oils. *SPE Journal, 3*(1), 54-61. doi:10.2118/37230-PA

Castor, T. P., Somerton, W. H., & Kelly, J. F. (1981). Recovery mechanisms of alkaline flooding. In D. O. Shah (Ed.), *Surface Phenomena in Ehanced Oil Recovery* (pp. 249-291). New York and London: Plenum Press.

Chilingar, G. V., & Yen, T. F. (1983). Some Notes on Wettability and Relative Permeabilities of Carbonate Reservoir Rocks, II. *Energy Sources, 7*(1), 67-75. doi:10.1080/00908318308908076

Cuiec, L. (1984). *Rock/Crude-Oil Interactions and Wettability: An Attempt To Understand Their Interrelation*. Paper presented at the SPE Annual Technical Conference and Exhibition, Houston, Texas.

Donaldson, E. C., & Alam, W. (2013). *Wettability*. Burlington: Elsevier Science.

Donaldson, E. C., Thomas, R. D., & Lorenz, P. B. (1969). Wettability Determination and Its Effect on Recovery Efficiency. doi:10.2118/2338-PA

Drummond, C., & Israelachvili, J. (2002). Surface forces and wettability. *Journal of Petroleum Science and Engineering, 33*(1), 123-133. doi:https://doi.org/10.1016/S0920-4105(01)00180-2

Emitech. (1999). Technical Brief; Sputter coating incoroporation Emitech K500, K550, K575 and K675X. Retrieved from https://crn2.3it.usherbrooke.ca/guide_sb/appareils/Emitech/SputterCoating.pdf

Fan, T., & Buckley, J. (2007). Acid number measurements revisited. *SPE J., 12*(4), 496-500.

Fathi, S. J., Austad, T., & Strand, S. (2010). "Smart Water" as a Wettability Modifier in Chalk: The Effect of Salinity and Ionic Composition. *Energy Fuels, 24*(4), 2514-2519. doi:10.1021/ef901304m

Fathi, S. J., Austad, T., & Strand, S. (2011). Water-Based Enhanced Oil Recovery (EOR) by "Smart Water": Optimal Ionic Composition for EOR in Carbonates. *Energy & Fuels, 25*(11), 5173-5179. doi:10.1021/ef201019k

Frykman, P. (2001). Spatial variability in petrophysical properties in Upper Maastrichtian chalk outcrops at Stevns Klint, Denmark. *Marine and Petroleum Geology, 18*(10), 1041-1062. doi:10.1016/S0264-8172(01)00043-5

Goldstein, J. I. (2003). *Scanning electron microscopy and X-ray microanalysis* (3rd ed. ed.). New York: Kluwer Academic/Plenum Publishers.

Green, D. W., & Willhite, G. P. (1998). *Enhanced oil recovery* (Vol. vol. 6). Richardson, Tex: Henry L. Doherty Memorial Fund of AIME, Society of Petroleum Engineers.

Hardman, R. F. P. (1982). *Chalk reservoirs of the North Sea*. Paper presented at the Bulletin of the Geological Society of Denmark Copenhagen, September 1st, 1982.

Hognesen, E. J., Strand, S., & Austad, T. (2005). *Waterflooding of preferential oil-wet carbonates: Oil recovery related to reservoir temperature and brine composition*. Paper presented at the SPE Europec/EAGE Annual Conference, Madrid, Spain.

Hopkins, P. A. (2016). *Water-based EOR and initial wettability in carbonates.* (Philosophiae Doctor Doctoral), University of Stavanger, Norway, University of Stavanger

Hopkins, P. A., Strand, S., Puntervold, T., Austad, T., Dizaj, S. R., Waldeland, J. O., & Simonsen, J. C. (2016). The adsorption of polar components onto carbonate surfaces and the effect on wetting. *Journal of Petroleum Science and Engineering, 147*, 381-387. doi:10.1016/j.petrol.2016.08.028

Lake, L. W. (2010). *Enhanced oil recovery*. Richardson, Tex: Society of Petroleum Engineers.

Lee, C.-H. (2010). *Experimental Investigation of Spontaneous Imbibition in Fractured Reservoirs*. Paper presented at the SPE Annual Technical Conference and Exhibition, Florence, Italy.

Lucia, F. J. (1999). *Carbonate reservoir characterization*. Berlin: Springer.

Ma, S. M., Zhang, X., Morrow, N. R., & Zhou, X. (1999). Characterization of Wettability From Spontaneous Imbibition Measurements. doi:10.2118/99-13-49

Madsen, L., & Lind, I. (1998). Adsorption of carboxylic acids on reservoir minerals from organic and aqueous phase. *SPE Reserv. Eval. Eng., 1*(1), 47-51.

Manrique, E., Muci, V., & Gurfinkel, M. (2007). EOR Field Experiences in Carbonate Reservoirs in the United States. *SPE Reservoir Evaluation & Engineering, 10*(6), 667-686. doi:10.2118/100063-PA

Mazzullo, S. J., Chilingarian, G. V., & Bissel, H. J. (1992). Carbonate rock classification. In S. J. Mazzullo, G. V. Chilingarian, & H. H. Rieke (Eds.), *Carbonate reservoir characterization: a geologic-engineering analysis: Pt. 1* (Vol. 30, pp. 59-108). Amsterdam: Elsevier.

Milter, J. (1996). *Improved oil recovery in chalk: spontaneous imbibition affected by wettability, rock framework and interfacial tension.* (Doctoral), Department of Chemistry, University of Bergen, Bergen.

Morrow, N. (1979). Interplay of Capillary, Viscous And Buoyancy Forces In the Mobilization of Residual Oil. *Journal of Canadian Petroleum Technology, 18*(3), 35-46. doi:10.2118/79-03-03

Morrow, N. R. (1990). Wettability and its effect on oil recovery. *JPT, Journal of Petroleum Technology, 42*(12), 1476-1484. doi:10.2118/21621-PA

Morrow, N. R., & Mason, G. (2001). Recovery of oil by spontaneous imbibition. *Current Opinion in Colloid & Interface Science, 6*(4), 321-337. doi:10.1016/S1359-0294(01)00100-5

Mousavi, M., Prodanovic, M., & Jacobi, D. (2013). New classification of carbonate rocks for process-based pore-scale modeling. *SPE Journal, 18*(2), 243-263. doi:10.2118/163073-PA

Norwegian Petroleum. (2018, 15.05.2018). The gorvernment revenues. Retrieved from https://www.norskpetroleum.no/en/economy/governments-revenues/

Pierre, A., Lamarche, J. M., Mercier, R., Foissy, A., & Persello, J. (1990). Calcium as potential determining ion in aqueous calcite suspensions. *Journal of Dispersion Science and Technology, 11*(6), 611-635. doi:10.1080/01932699008943286

Puntervold, T. (2008). *Waterflooding of carbonate reservoirs: EOR by wettability alteration.* (Philosophiae Doctor Doctoral), University of Stavanger, Norway.

Puntervold, T., Strand, S., & Austad, T. (2007a). New Method To Prepare Outcrop Chalk Cores for Wettability and Oil Recovery Studies at Low Initial Water Saturation. *Energy & Fuels, 21*(6), 3425-3430. doi:10.1021/ef700323c

Puntervold, T., Strand, S., & Austad, T. (2007b). Water flooding of carbonate reservoirs: Effects of a model base and natural crude oil bases on chalk wettability. *Energy Fuels, 21*(3), 1606-1616. doi:10.1021/ef060624b

Ravari, R. R. (2011). Water-Based EOR in Limestone by Smart Water : A study of surface chemistry: University of Stavanger, Norway.

Rezaeidoust, A., Puntervold, T., Strand, S., & Austad, T. (2009). Smart Water as Wettability Modifier in Carbonate and Sandstone: A Discussion of Similarities/Differences in the Chemical Mechanisms. *Energy Fuels, 23*(9), 4479-4485. doi:10.1021/ef900185e

Rogen, B., & Fabricius, I. L. (2002). Influence of clay and silica on permeability and capillary entry pressure of chalk reservoirs in the North Sea. *Petroleum Geoscience, 8*(3), 287-293. doi:10.1144/petgeo.8.3.287

Salathiel, R. A. (1973). Oil Recovery by Surface Film Drainage In Mixed-Wettability Rocks. doi:10.2118/4104-PA

Shariatpanahi, S. F. (2012). *Improved waterflood oil recovery from carbonate reservoirs: a wettability alteration process.* (Philosophiae Doctor Doctoral), University of Stavanger, Stavanger.

Shariatpanahi, S. F., Hopkins, P., Aksulu, H., Strand, S., Puntervold, T., & Austad, T. (2016). Water Based EOR by Wettability Alteration in Dolomite. *Energy and Fuels, 30*(1), 180-187. doi:10.1021/acs.energyfuels.5b02239

Shariatpanahi, S. F., Strand, S., & Austad, T. (2011). Initial wetting properties of carbonate oil reservoirs: Effect of the temperature and presence of sulfate in formation water. *25*(7), 3021-3028. doi:10.1021/ef200033h

Skinner, B. J., & Porter, S. C. (1992). *The dynamic earth : an introduction to physical geology* (2nd ed. ed.). New York: Wiley.

Smart water group, Institute of Energy resources., UiS. (2018). *An introduction to "Smart Water" in Carbonates*. Canvas.

Speight, J. G. (2004). Petroleum Asphaltenes - Part 1: Asphaltenes, Resins and the Structure of Petroleum. *Oil & Gas Science and Technology - Rev. IFP, 59*(5), 467-477.

Speight, J. G. (2014). *The chemistry and technology of petroleum* (5th ed. ed. Vol. 137). Boca Raton, Fla: CRC Press.

Springer, N., Korsbeck, U., & Aage, K. H. (2003). *Resistivity index measurement without the porous plate: A desaturation technique based on evaporation produces uniform water saturation profiles and more reliable results for tight North Sea chalk*. Paper presented at the The International Symposium of the Society of Core Analysts Pau, France.

Standnes, D. C., & Austad, T. (2000). Wettability alteration in chalk: 1. Preparation of core material and oil properties. *Journal of Petroleum Science and Engineering, 28*(3), 111-121. doi:10.1016/S0920-4105(00)00083-8

Strand, S. (2005). *Wettability alteration in chalk: a study of surface chemistry*. (Philosophiae Doctor Doctoral), University of Stavanger, Stavanger.
Strand, S., Puntervold, T., & Austad, T. (2016). Water based EOR from clastic oil reservoirs by wettability alteration: A review of chemical aspects. *Journal of Petroleum Science and Engineering, 146*, 1079-1091. doi:10.1016/j.petrol.2016.08.012
Strand, S., Standnes, D. C., & Austad, T. (2006). New wettability test for chalk based on chromatographic separation of SCN^- and SO_4^{2-}. *Journal of Petroleum Science and Engineering, 52*(1-4), 187-197. doi:10.1016/j.petrol.2006.03.021
Treiber, L. E., Archer, D. L., & Owens, W. W. (1972). A Laboratory Evaluation of the Wettability of Fifty Oil-Producing Reservoirs. doi:10.2118/3526-PA
Zhang, P. (2006). *Water-based EOR in fractured chalk: wettability and chemical additives*. (Philosophiae Doctor Doctoral), University of Stavanger, Norway, Stavanger.
Zhang, P., & Austad, T. (2005). *The Relative Effects of Acid Number and Temperature on Chalk Wettability*. Paper presented at the SPE International Symposium on Oilfield Chemistry, The Woodlands, Texas.
Zhang, P., Tweheyo, M. T., & Austad, T. (2007). Wettability alteration and improved oil recovery by spontaneous imbibition of seawater into chalk: Impact of the potential determining ions Ca^{2+}, Mg^{2+}, and SO_4^{2-}. *Colloids and Surfaces A: Physicochemical and Engineering Aspects, 301*(1), 199-208. doi:10.1016/j.colsurfa.2006.12.058
Zolotuchin, A. B., & Ursin, J.-R. (2000). *Introduction to petroleum reservoir engineering*. Kristiansand: Høyskoleforlaget AS.

Appendix A: Chemicals

A.1 Acid number solutions

Table 10: Chemicals for AN measurements

Solution	Chemicals	Formula	Description
Titrant	KOH (>85%) 2-propanol	KOH $CH_3CHOHCH_3$	2.8 g KOH (>85%) dilute to 1000 ml with 2-propanol ($CH_3CHOHCH_3$)
Spiking solution	Stearic acid Acid titration solvent	$CH_3(CH_2)_{16}COOH$	0.5 g Stearic Acid – $CH_3(CH_2)_{16}COOH$ dilute to 100 ml with Acid titration solvent
Standard solution	Potassium Hydrogen Phtalate, KHP DI water	$HOOCC_6H_4COOK$	0.2 g Potassium Hydrogen Phtalate, KHP diluted to 500 ml with DI water
Titration solvent	DI water 2-propanol Toulene	 $CH_3CHOHCH_3$ $C_6H_5CH_3$	6 ml DI water dilute with 494 ml 2-propanol and with 500 ml Toulene
Electrode/ Electrolyte	Potassium chloride DI water	KCl	Mettler DG-114 Electrode 3 M KCl in DI water

A.2 Base number solutions

Table 11: Chemicals for BN measurements

Solution	Chemicals	Formula	Description
Titrant	Perchloric Acis (70%) Acetic Anhydride Acetic Acid	$HClO_4$ (70%) $(CH_3CO)_2O$ CH_3COOH	5 ml 70% Percholric Acid ($HClO_4$) 15 ml Acetic Anhydride ($(CH_3CO)_2O$) dilute to 1000 ml with Acetic Acid (CH_3COOH)
Spiking solution	Quinoline Decane	C_9H_7N $CH_3(CH_2)_8CH_3$	0.5 g Quinoline (C_9H_7N) dilute to 100 ml with Decane ($C_{10}H_{22}$)
Standard solution	Potassium Hydrogen Phtalate, KHP Acetic Acid	$HOOCC_6H_4COOK$ CH_3COOH	0.2 g Potassium Hydrogen Phtalate, KHP diluted to 250 ml with Acetic Acid CH_3COOH
Titration solvent	Methyl Isobutyl Ketone, MIKB	$(CH_3)_2CHCH_2COCH_3$	Methyl Isobutyl Ketone (MIBK), ($(CH_3)_2CHCH_2COCH_3$)
Electrode/ Electrolyte	Sodium Perchlorate, (solid) 2-propanol	$NaClO_4$ (S) $CH_3CHOHCH_3$	Mettler DG-113 Electrode Electrolyte: Saturated Sodium Perchloride, ($NaClO_4$ (s)), in 2-propanol

Appendix B: Experimental data

B.1 Acid and base numbers

Table 12: BN values for core A2

PV corrected	BN
0.839106377	0.13
0.922198483	0.25
1.149109822	0.22
1.250218161	0.23
1.348375564	0.22
1.445911718	0.24
1.54329256	0.23
1.737743618	0.26
1.933281864	0.32
2.290500262	0.28
2.387570479	0.28
2.485106633	0.32
2.58217685	0.29
2.679091755	0.3
2.776472597	0.29
2.973563965	0.3
3.171431896	0.31
3.3702317	0.29
3.571982439	0.28
3.672469528	0.33
3.772024742	0.33
3.861950592	0.29

Table 13: AN values for core A2

PV corrected	AN
0.839106377	0.02
0.922198483	0.02
1.058407412	0
1.149109822	0.07
1.250218161	0.06
1.640362777	0.07
1.835435085	0.06
2.03097333	0.06
2.290500262	0.01
2.485106633	0.03
2.679091755	0
3.072497931	0
3.471029414	0.01
3.672469528	0.01
3.861950592	0.07

Table 14: Estimation of adsorbed bases, core A2

PV	C/C0	Area under curve
0	0	
0.839106377	0.13	0.054541915
0.922198483	0.25	0.0157875
1.149109822	0.22	0.053324165
1.250218161	0.23	0.022749376
1.348375564	0.22	0.022085416
1.445911718	0.24	0.022433315
1.54329256	0.23	0.022884498
1.737743618	0.26	0.047640509
1.933281864	0.32	0.056706091

Area under curve	0
Area of "box"	0.012386532
Adsorption area	0.012386532

Table 15: BN values for core A3

PV corrected	BN
0.83658653	0.1
0.9172226	0.25
1.019835951	0.26
1.085609687	0.24
1.230122173	0.34
1.356452016	0.32
1.538594668	0.31
1.88074458	0.3
2.184157557	0.3
2.3835285	0.34
2.688212048	0.35
3.389903966	0.31
3.589280602	0.31
3.88953138	0.25
3.990089302	0.25

Table 16: AN values for core A3

PV corrected	AN
0.83658653	0
0.9172226	0.11
1.085609687	0.07
1.230122173	0.11
1.356452016	0
1.462385676	0.07
1.624922695	0.03
1.781609647	0
1.88074458	0.01
2.184157557	0
2.688212048	0.06
3.088230199	0.07
3.489987559	0.03
3.88953138	0.05
4.089856675	0.08

Table 17: Estimation of adsorbed bases, core A3

PV	C/C0	Area under curve
0	0	
0.83658653	0.1	0.041829326
0.9172226	0.25	0.014111312
1.019835951	0.26	0.026166405
1.085609687	0.24	0.016443434
1.230122173	0.32	0.040463496

Area under curve	0.139013973
Area of box	0.4
Adsorption area	0.260986027

B.2 Spontaneous and forced imbibition data

Table 18: SI data, reference core

Time (Days)	Volume of Heptane (ml)	OOIP %
0.0000	0	0.00
0.0014	8.4	24.31
0.0021	10.1	29.23
0.0028	12.6	36.47
0.0035	15.8	45.73
0.0104	20.5	59.33
0.0139	22	63.68
0.0174	22.5	65.12
0.0229	23	66.57
0.0278	23.4	67.73
0.0319	23.5	68.02
0.0347	23.7	68.60
0.0417	23.8	68.89
0.0625	24.1	69.75
0.0833	24.2	70.04
0.1250	24.3	70.33
0.1667	24.4	70.62
1.0000	24.4	70.62
2.0000	24.6	71.20
3.0069	24.6	71.20
4.125	24.6	71.20
15	24.6	71.20

Table 19: SI and FI data, core A2

Time	Time (Days)	ml	%OOIP	
Ref. time(11:00)Start	0	0	0	
30 min	0.020833333	0	0	
1 hours	0.041666667	0	0	
2 h	0.083333333	1	2.855079043	
3 h	0.125	3.1	8.850745033	
3 1/2 h	0.145833333	3.8	10.84930036	
4 h	0.166666667	4.5	12.84785569	
5 1/2 h	0.208333333	7.2	20.55656911	
12 h	0.5	11.4	32.54790109	
1 day	1	13.6	38.82907498	
2 d	2	14.7	41.96966193	
3 d	3	15.9	45.39575678	
4 d	4	16.8	47.96532792	
5 d	5	17.4	49.67837535	
6 d	6	17.6	50.24939115	
7 d	7	17.8	50.82040696	
8 d	8	18.1	51.67693068	
9 d	9	18.4	52.53345439	
10 d	10	18.5	52.81896229	
11 d	11	18.50	52.81896229	
11 d 2 h	11.08333333	18.5	52.81896229	
11 d 2 1/2 h	11.10416667	18.6	53.1044702	**FI start 1 PV/d**
11 d 3 1/2 h	11.14583333	19.65	56.10230319	
11 d 4 1/2 h	11.1875	21.3	60.81318361	
11 d 6 1/2 h	11.27083333	21.4	61.09869152	
12 d	12	21.4	61.09869152	
13 d	13	21.4	61.09869152	
14 d	14	21.4	61.09869152	**FI start 4 PV/d**
14 d 1h	14.04166667	21.5	61.38419942	
14 d 2h	14.08333333	21.6	61.66970733	
14 d 4h	14.16666667	21.7	61.95521523	
14 d 4h	14.16666667	21.7	61.95521523	
14 d 6 1/2 h	14.27083333	21.7	61.95521523	
14 d 20 h	14.83333333	21.8	62.24072313	
14 d 22h	14.91666667	21.8	62.24072313	

Table 20: SI and FI data, core A3

Time	Time (Days)	ml	%OOIP	
Ref. time (09:00)Start	0	0	0	
2 hours	0.083333333	0.3	0.839292309	
2 1/2 h	0.104166667	0.6	1.678584617	
3 h	0.125	1.4	3.916697441	
3 1/2 h	0.145833333	1.8	5.035753852	
4 h	0.166666667	2.2	6.154810264	
1 day	1	12.4	34.69074876	
2 d	2	14.9	41.68485133	
3 d	3	16.8	47.00036929	
4 d	4	17.5	48.95871801	
5 d	5	18	50.35753852	
6 d	6	18.4	51.47659494	
7 d	7	18.5	51.75635904	
8 d	8	18.7	52.31588724	
9 d	9	18.8	52.59565135	
10 d	10	18.9	52.87541545	
11 d	11	18.9	52.87541545	
11d 6 1/2 h	11.27083333	19	53.15517955	**FI start, 1 PV/d**
11 d 7 h	11.29166667	19.3	53.99447186	
11 d 8 h	11.33333333	19.4	54.27423596	
11 d 21 h	11.875	19.8	55.39329238	
12 d 1 1/2 h	12.0625	19.8	55.39329238	
12 d 3 1/2 h	12.14583333	19.9	55.67305648	
12 d 8 h	12.33333333	19.9	55.67305648	
12 d 20 h	12.83333333	20	55.95282058	
12 d 22 h	12.91666667	20.1	56.23258468	
13 d 2 h	13.08333333	20.2	56.51234879	
13 d 8 h	13.33333333	20.2	56.51234879	
13 d 21 1/2 h	13.89583333	20.2	56.51234879	
14 d 1 h	14.04166667	20.2	56.51234879	**FI start, 4 PV/d**
14 d 5 1/2 h	14.22916667	20.8	58.1909334	
14 d 7 h	14.29166667	21	58.75046161	
14 d 8 1/2 h	14.35416667	21.2	59.30998982	
14 d 19 h	14.79166667	21.2	59.30998982	
15 d	15	21.2	59.30998982	

B.3 Chromatography data

Table 21: Chromatography data, reference core

Thiocyanate		
PV	C/C0	Area under curve
0.78	0	
0.90	0.089978054	0.005600486
1.03	0.636430139	0.045400512
1.15	0.967812729	0.099852565
1.28	0.998536942	0.122138232
1.40	0.994147769	0.124542794
1.53	0.996342356	0.123381718
1.65	1.031455743	0.126476605
1.78	1.000731529	0.126489023

Sulfate		
PV	C/C0	Area under curve
0.90	0	
1.03	0.0319503	0.0020
1.15	0.234302197	0.0166
1.28	0.612380741	0.0526
1.40	0.764144664	0.0860
1.53	0.862658087	0.1008
1.65	0.917239849	0.1110
1.78	0.966496561	0.1172

Total area thiocyanate	Total area sulfate	Area in between two curves
0.7739	**0.4863**	**0.2876**

Table 22: Chromatography data, core A2

Thiocyanate		
PV	C/C0	Area under curve
0.36	0	
0.49	0.071805702	0.004621341
0.62	0.369588173	0.028520835
0.75	0.671594509	0.067276419
0.88	0.8468849	0.097922454
1.01	0.944033791	0.1157209
1.14	0.992608237	0.125633444
1.27	0.97782471	0.127572902
1.40	1.001055966	0.128119839
1.52	0.998944034	0.128974359
1.65	0.984160507	0.127884818
1.78	0.975712777	0.126637966

Sulfate		
PV	C/C0	Area under curve
0.62	0	
0.75	0.204350315	0.0132
0.88	0.450104942	0.0422
1.01	0.657126503	0.0715
1.14	0.782675062	0.0934
1.27	0.922915474	0.1104
1.40	0.964319786	0.1222
1.52	0.980347262	0.1254
1.65	0.956306048	0.1249
1.78	0.999045984	0.1263

Total area thiocyanate	Total area sulfate	Area in between two curves
1.0789	**0.8296**	**0.2493**

Table 23: Chromatography data, core A2

Thiocyanate		
PV	C/C0	Area under curve
0.40	0	
0.52	0.31380978	0.02018427
0.65	0.707146695	0.065409468
0.78	0.846856529	0.099363336
0.91	0.997313272	0.117683158
1.68	0.982267598	0.759699876
1.75	1.00304013	0.06948577

Sulfate		
PV	C/C0	Area under curve
0.47	0	
0.59	0.092217268	0.0059
0.72	0.201459262	0.0188
0.85	0.466761248	0.0427
0.98	0.771787596	0.0790
1.11	0.936359951	0.1097
1.23	0.951965951	0.1207
1.75	1.00304013	0.4998

Total area thiocyanate	Total area sulfate	Area in between two curves
1.1318	**0.8767**	**0.2552**